



Andean berry (*Vaccinium meridionale* Swartz) juice, in combination with Aspirin, displayed antiproliferative and pro-apoptotic mechanisms *in vitro* while exhibiting protective effects against AOM-induced colorectal cancer *in vivo*

Sandra S. Arango-Varela^{a,*}, Ivan Luzardo-Ocampo^{b,c}, Maria E. Maldonado-Celis^d

^a Biomedical Research and Innovation Group (GI2B), Instituto Tecnológico Metropolitano (ITM), Medellín, Colombia

^b Instituto de Neurobiología, Universidad Nacional Autónoma de México, Juriquilla, Mexico

^c Research and Graduate Program in Food Science, Universidad Autónoma de Querétaro, Queretaro, Mexico

^d Escuela de Nutrición y Dietética, Universidad de Antioquia, Medellín, Colombia

ARTICLE INFO

Keywords:

Vaccinium meridionale Swartz
Aspirin
Azoxymethane
Colon cancer
Phenolic compounds

ABSTRACT

Colorectal cancer (CRC) can be either prevented or alleviated using conventional drugs combined with natural treatments. Andean berry (AB, *Vaccinium meridionale* Sw.) is an underutilized berry with promising anti-inflammatory and antiproliferative effects that could be used to alleviate CRC markers in combination with Aspirin, a well-known CRC preventive drug. This research aimed to evaluate the impact of Aspirin, AB juice (ABJ), and their mixture on colorectal cancer *in vitro* and *in vivo*. The treatments (ABJ: 0, 10, 20, and 30 % v/v; Aspirin: 0, 10, 15, and 20 mM; and their combination) were assessed on SW480 cells to test their antiproliferative and pro-apoptotic effect. To evaluate their chemopreventive and chemoprotective effect *in vivo*, azoxymethane (AOM, 15 mg/kg BW) was used as a chemical inductor of early-stage colon cancer. Balb/c mice (8 weeks' age) were randomly assigned to five groups (n = 6 mice/group): control (no treatment), positive control (AOM-treated mice), AOM + Aspirin (20 mM: 25 mg/kg BW), AOM + ABJ (30 % v/v), and AOM + Aspirin + ABJ (Aspirin: 25 mg/kg BW; ABJ: 30 % v/v). ABJ contained phenolic compounds such as 3,4-dihydroxybenzoic and gallic acids, morin, and rutin. The mixture showed a strongest antiproliferative effect than their counterparts (+10.39–46.23 %). Except for Aspirin (20 mM), the cells were not able to proliferate based on the cloning efficiency test. The mixture was the most effective treatment arresting the cell cycle and increasing G2/M cell population ($p < 0.01$). Aspirin and ABJ showed mainly intrinsic and extrinsic-mediated apoptotic processes, while the mixture decreased most pro-apoptotic (cytochrome C, DR4, DR5, TNFRSF1A, Bax, and Bad) and anti-apoptotic proteins (Hsp70, Hsp32, and XIAP) compared to the untreated cells. *In silico* simulations highlighted the interaction between rutin and catalase as the strongest affinity (−10.30 Kcal/mol). ABJ and the mixture decreased aberrant crypt foci *in vivo* compared to AOM-only treated mice and protected the colonic and liver architecture, this was latter used as a secondary indicator of AOM-metabolic activity. The chemopreventive approach was more effective, related to a prior regulation of cancer-protective mechanisms *in vivo*, alleviating the AOM-induced damage. The results indicated that Aspirin and ABJ mixtures exhibit antiproliferative and pro-apoptotic effects in SW480 cells inducing mechanisms linked to extrinsic (TNF and TRAIL-mediated apoptosis)

Abbreviations: ABJ, Andean berry (*Vaccinium meridionale* Swartz) juice; ACF, Aberrant crypt foci; AOM, Azoxymethane; BCA, Bicinchoninic acid; BW, Body weight; CE, Cloning efficiency; COX-2, Cyclooxygenase-2; CRC, Colorectal cancer; DAD, Diode array detector; DMH, 1,2-dimethylhydrazine; DMEM, Dulbecco's Modified Eagle Medium; DSS, Dextran sodium sulfate; H&E, Hematoxylin and eosin; HIF-1 α , Hypoxia-inducible factor 1 α ; HPLC, High-performance liquid chromatography; HS, Horse serum; Hsp32, Heat-shock protein 32; IC₅₀, Concentration at which 50 % viability is reached; ITS, Insulin, transferrin, and selenium medium; KEGG, Kyoto Encyclopedia of Genes and Genomes; NLRP3, Nucleotide-binding oligomerization domain-like receptor 3; NSAIDs, Non-steroidal anti-inflammatory drugs; OD, Optical density; RCE, Relative cloning efficiency; PARP, Poly (ADP-ribose) polymerase; PBMCs, Peripheral blood mononuclear cells; PI, Propidium iodide; RLU, Relative luminescent units; ROS, Intracellular reactive oxygen species; SRB, Sulphorhodamine B; STAT, Signal transducer and activator of transcription; TCA, Trichloroacetic acid; TLR4, Toll-like receptor 4; TRAIL1, TNF-related apoptosis-inducing ligand receptor; VEGF, Vascular endothelial growth factor; WCE, Whole cranberry (*Vaccinium macrocarpon*) extract; XIAP, X-linked inhibitor of apoptosis.

* Corresponding author at: Cra. 65 #98A-75, Medellín, Antioquia, Colombia.

E-mail address: sandraarango@itm.edu.co (S.S. Arango-Varela).

<https://doi.org/10.1016/j.foodres.2022.111244>

Received 23 March 2021; Received in revised form 8 April 2022; Accepted 9 April 2022

Available online 12 April 2022

0963-9969/© 2022 The Authors. Published by Elsevier Ltd. This is an open access article under the CC BY-NC-ND license (<http://creativecommons.org/licenses/by-nc-nd/4.0/>).

and intrinsic (Bax and cytochrome C modulation) pathways. At *in vivo* levels, the treatments displayed defensive effects against the AOM-induced damage as observed by macroscopic measurements. However, more *in vitro*, and *in vivo* approaches are required to completely fulfill the pro-apoptotic, anti-proliferative, and chemopreventive/chemoprotective effects of ABJ.

1. Introduction

Colorectal cancer (CRC) is one of the leading cancer types in mortality, starting when certain cell types from the intestinal epithelium acquire genetic and epigenetic mutations, conferring a selective hyper-proliferative advantage with potential evolution to carcinoma and metastasis (Mattiuzzi et al., 2019). As such, CRC remains the third more common malignant condition worldwide, carrying considerable side effects, a saturation of health care services, and high medical costs (Wong et al., 2021). An emerging interest in comprehending several strategies controlling CRC includes diet and lifestyle changes, antioxidants administration, and chemoprevention, aiming to prevent adenoma growing and its further development (López et al., 2014). This prevention relies on monitoring uncontrolled proliferation as a key cell process for its development and inducing apoptosis in cancer cells (Goldar et al., 2015). Chemoprevention is also supported by the synergistic activity of phytochemicals, either alone or combined with chemotherapeutic agents, providing a potentiate anticancer activity and diminishing side effects from drug treatments (Patra et al., 2021).

Among the CRC chemopreventive strategies, substantial evidence has been shown for non-steroidal anti-inflammatory drugs (NSAIDs) such as Aspirin, mainly on its inhibitory effects on cancer cell growth and pro-apoptotic induction mechanisms suppressing the anti-apoptotic protein Bcl-2 and up-regulating the levels of cleaved PARP and Bax (Jiang et al., 2020), delay cell proliferation, and promotes cell cycle arrest at G0/G1 stages (Drew et al., 2016). *in vitro*. Moreover, Aspirin induces DNA repair and suppresses colon formation in the Azoxymethane colon tumor model (Rohwer et al., 2020) and effectively decrease the metastatic ability of colon cancer cells, downregulating toll-like receptor 4 (TLR4) and the NF- κ B pathway (Ying et al., 2018).

Aspirin therapy can be combined with natural products to reduce NSAIDs' use and their adverse side effects, such as gastrointestinal and cardiovascular toxicity (Sharma et al., 2020). For this goal, Andean Berry (*Vaccinium meridionale* Swartz) might be a suitable alternative since this fruit contains several phytochemicals, mainly phenolic compounds (Agudelo, Luzardo-Ocampo, Campos-Vega, Loarca-Piña, & Maldonado-Celis, 2018). Andean berry (*Vaccinium meridionale* Swartz) is a berry known as "mortiño" or "agraz" belonging to the *Ericaceae* family, commonly cultivated in the Andean region of South America (Ligarreto et al., 2011). This underutilized fruit offers a high variety of phytochemicals exhibiting a wide range of bioactive properties (Garzón, 2012). Unfortunately, the low production of this fruit and the heterogeneous conditions at which is cultivated is still a challenge to promote its consumption and research focused on its health-promoting potential (Maldonado-Celis et al., 2017). Particularly for Andean berry, pro-apoptotic and antiproliferative effects have been reported *in vitro* in transformed leukemic and colorectal cancer cell lines (González et al., 2017; Zapata et al., 2020).

To explain the anticancer mechanisms, phenolics from *V. meridionale* have been linked to cell proliferation inhibition due to their antioxidant properties, modulating molecular targets (Jingwen et al., 2017). Phenolic compounds can induce pro-apoptotic events such as activating proteins like caspase-3 and caspase-9 and participating in cytochrome c release as Bax and Bak activation and the modulation of NF- κ B, among other processes (D'Archivio et al., 2008; Szliszka & Krol, 2011).

Together with *in vitro* tests, preclinical evaluation of therapies must consider *in vivo* assays. Some chemical inductors of CRC are 1,2-dimethylhydrazine (DMH) or azoxymethane (AOM). The repeated administration of AOM contributes to developing epithelial neoplasia initiated

at abnormal colonic crypts or aberrant crypt foci (ACF) (Orlando et al., 2008). Researchers have reported both chemoprotective and chemopreventive effects from berry fruits, underlining the most beneficial effects to phenolic compounds (Baby et al., 2018). Surprisingly, there is no evidence of *in vivo* chemopreventive or chemoprotective evaluations of Andean berry rather than a previous report indicating the ability of this fruit to improve plasma antioxidant capacity and IL-6 levels in healthy people with a dietary risk of developing colorectal cancer (Agudelo, Ceballos, Gómez-García, & Maldonado-Celis, 2018).

The evaluation of the efficacy and efficiency of drugs require their test separately and combined to consider their effects in both conditions (Landis-piwowar & Iyer, 2014). Hence, this study aimed to evaluate the impact of the combined Andean berry juice (ABJ) and Aspirin treatment on colorectal cancer *in vitro* and *in vivo*. We hypothesized that the combination of both treatments would produce an antiproliferative and pro-apoptotic effect *in vitro* on the human colorectal adenocarcinoma SW480 cell line while reducing aberrant crypt foci formation and colonic damage *in vivo*. This is the first report of a chemopreventive and chemoprotective evaluation approach *in vivo* combining ABJ and Aspirin.

2. Materials and methods

2.1. Andean Berry collection and juice preparation

Ripe Andean berry (*Vaccinium meridionale* Swartz) berries were collected in the municipality of El Retiro (Antioquia, Colombia) at 2175 m above the sea level (6° 8' 6"N; 75° 25' 3" W) and 16 °C of average temperature. The specimens were identified by the herbarium from the University of Antioquia (National Registry of Biological Collections #027). The berries were washed, disinfected (sodium hypochlorite, 100 ppm), dried, and ground (2500 rpm, 2 min) using a commercial blender (KB720-5, KRUPS, Solingen, Germany). The product was then freeze-dried (0.427 ± 0.50 mm Hg, -50 °C) in a vacuum chamber (FreeZone 4.5, Labconco, Kansas City, MO, US) and stored protected from light in polyethylene terephthalate packages (200 g each one).

The Andean berry juice (ABJ) was prepared as informed by Franco-Tobón et al. (2016). Briefly, the freeze-dried powder was dissolved in a 10 % v/v sucrose/water solution to obtain a juice with 11 °Brix and 4.33 mg citric acid/mL (pH: 3.06). The mixture was sonicated in a Branson sonicator (B3510, Ultrasonic Corporation, Boston, MA, US) at 42 kHz and 135 W, filtered (0.22 μ m filter), and the juice was stored in the dark at -20 °C until use.

2.2. Extraction, identification, and quantification of the free phenolic compound's composition of ABJ by HPLC-DAD

Free (extractable or unbound) phenolic compounds were extracted, as reported by Arango-Varela, Luzardo-Ocampo, Maldonado-Celis, & Campos-Vega (2020). ABJ was mixed with high-performance liquid chromatography (HPLC)-grade methanol in a 1:10 proportion, and the solution was stirred for 24 h in a 50 mL-flask, protected from light, at room temperature (25 ± 1 °C). The solution was then centrifuged (2166g, 10 min, 4 °C) in a Hermle Z233 K centrifuge (Hermle, Gosheim, Baden-Württemberg, Germany), and supernatants were collected and filtered through a sterile 0.45 μ m filter (acrodisc syringe filters, Agilent, Palo Alto, CA, US). The filtered solution was stored at -20 °C, protected from light until use.

The phenolic compounds' composition of ABJ was determined

following the procedure of Ramírez-Jiménez, Reynoso-Camacho, Mendoza-Díaz, & Loarca-Piña (2014) with slight modifications. For this, an Agilent 1100 Series HPLC (Agilent Technologies) coupled to a diode array detector (DAD) (Agilent Technologies) was used. The chromatographic separation was carried out in a Zorbax Eclipse C18 column (4.6 × 250 mm, 5 µm; Agilent Technologies) in a 1 mL/min gradient combining two solvents as mobile phase: acetic acid 1 % v/v with water (solvent A) and 100 % acetonitrile (solvent B). A linear gradient was used as follows: 80–83 % A for 15 min, 83–60 % 83–60 % A for 15 min, 60–50 % for 5 min, 50–85 % for 5 min. The detection was performed at 280 nm for phenolic acids and 320 nm for flavonoids in thermostatically controlled conditions for the column (35 ± 0.6 °C), using an injection volume of 20 µL and an acquisition speed of 1 s. The amount of phenolic compounds was determined by comparison with standard curves (0.125, 0.250, 0.500, 0.750, and 1.000 mg/mL) of HPLC-grade standards of gallic (27645), chlorogenic (C3878), caffeic (C0625), ellagic (E2250), p-coumaric (C9008); 3,4-hydroxybenzoic (240141), and 2-hydroxycinnamic acids (H22809) as phenolic acids (Sigma-Aldrich, St. Louis, MO, US). As flavonoids, (+)-catechin (C1251), rutin (R5143), morin (PHL82601), and kaempferol (60010) were used (Sigma-Aldrich, St. Louis, MO, US). The results were expressed as micrograms equivalents of each phenolic compound by gram of ABJ. All solvents were HPLC-grade and acquired from J. T. Baker (Mexico City, Mexico). Additional information about the analytical method is provided in **Supplementary Table S1**.

2.3. *In vitro* assays

Human SW480 (European Collection of Animal Cell Culture, ECACC 87092801) colon adenocarcinoma cells were cultured in Dulbecco's Modified Eagle Medium (DMEM) (Gibco, Invitrogen, Carlsbad, USA) supplemented with 25 mM glucose, 2 mM L-glutamine, 10 % horse serum (HS, Gibco, Invitrogen, Carlsbad, US), 100 UI/mL penicillin, 100 µg/mL streptomycin, and 1 % of non-essential amino acids (Gibco, Invitrogen). Cells were maintained in humidified 5 % CO₂ atmosphere at 37 °C. For the experiments, medium supplemented with 3 % horse serum, Insulin-Transferrin-Selenium (ITS) supplement, 10 µg/mL insulin, 5 µg/mL transferrin, and 5 ng/mL selenium (Gibco, Invitrogen, Carlsbad, US) were used.

2.3.1. Antiproliferative analysis by Sulphorhodamine B (SRB) test

To evaluate the antiproliferative effect of the ABJ and Aspirin on SW480 cells, the SRB assay was used, measuring the optical density (OD) of the bound colorant to the cell membranes after the treatment (Vichai & Kirtikara, 2006). Cell cultures with viability higher than 95 % were used for this test. The cells (2.5 × 10⁴ cells/well, 100 µL) were seeded with ITS-supplemented medium on 96-well plates for 24 h. Then, medium was replaced by ABJ treatments (10, 20, and 30 % v/v), Aspirin (10, 15, and 20 mM) (70264–013, Bayer-Leverkusen, Germany), and the ABJ + Aspirin mixture (30 % v/v ABJ + Aspirin 20 mM) for several incubation times (0, 24, 48, and 72 h). The doses were selected based on a previous report from our research group indicating that ABJ concentrations up to 30 % v/v did not exhibit cytotoxic effects on RAW 264.7 (Arango-Varela et al., 2020), whereas the calculated IC₅₀ (24 or 48 h) for Aspirin was close to 20 mM, a similar dose to those already tested for several cancer cell lines. The treatments were reconstituted each 48 h to avoid its dryness. At the end of the incubation period, treatments were replaced with trichloroacetic acid (10 % TCA, 100 µL) and incubated at 4 °C for 1 h. After acid removal, SRB (0.4 % v/v) was added and incubated for 30 min at room temperature (25 ± 1 °C). Plates were washed with TCA 1 % (J. T. Baker) and let dry at room temperature for 24 h. The SRB was solubilized, adding 200 µL of Tris-HCl (10 mM, pH: 10.5) buffer for 20 min. OD was quantified at 490 nm in a plate reader (GloMax® Multi Microplate Reader, Molecular Devices, Sunnyvale, CA, US). This assay was carried out three times using 5 replicates for treatment. The results were expressed as cell viability (%) against the control:

$$[\text{OD}_{\text{sample}}/\text{OD}_{\text{Control}}] \times 100 \%$$

The concentration at which 50 % viability was reached (IC₅₀) was calculated using a statistical regression curve provided by GraphPad Prism v. 9.0 software.

2.3.2. Clonogenic assay

The clonogenic assay was performed to determine the proliferative capacity of the cells exposed to the treatments, as reported by Franken, Rodermond, Stap, Haveman, & van Bree (2006) with slight modifications. In the exponential phase, cells (150 cells/well) were inoculated in 12-well plates (2 mL of final volume) with ITS-supplemented medium. The medium was then replaced with Aspirin (20 mM), ABJ (30 %), or their combination for 24 h. The samples were incubated for 7 days with ITS medium, being replaced each 48 h to avoid dryness. After the incubation, the medium was removed, cells were washed with PBS 1×, and the cells were fixed with Carnoy's solution (1:3 methanol: acetic acid) (J. T. Baker) and stained with crystal violet (0.5 % m/v) for 10 min. The number of established colonies (50 or more cells/colony) was count in an inverted microscope. This assay was conducted in triplicates, and the results were used to calculate the cloning efficiency (CE): [Number of colonies from the treatment/Number of colonies from the control] * 100 %. The CE value was then used to calculate the relative cloning efficiency (RCE): [CE_{treatment} / CE_{control}] * 100 %.

2.3.3. Cell cycle distribution determination by flow cytometry

The cell cycle distribution was carried out using DNA staining with propidium iodide (PI) (Ramirez et al., 2019). The cells (1 × 10⁶ cells/well) were seeded on 6-well plates for 24 h. Then, the cells were treated with 20 mM Aspirin, 30 % ABJ, or their combination. The cells were trypsinized (trypsin 1×, Gibco, US) (100 µL/well), and an aliquot was fixed with 96 % v/v ethanol (2 mL) (J. T. Baker). The cell suspensions were stored at –20 °C for 24 h and were then washed with PBS 1 ×. The fixed cells were resuspended in 500 µL PBS supplemented with 250 µL RNase and 10 µL PI. The cells were incubated at room temperature for 30 min in the dark. The flow cytometry assay (FACSCanto™ II, BD Biosciences, Franklin Lakes, NJ, US) analyzed 10,000 events per sample at 488/530 nm excitation and detection wavelengths using green filters.

2.3.4. Caspase-3/7 activity measurement

The caspase-3/7 activity assay was estimated with the ApoTox-Glo™ Triplex Assay (Promega Corporation, Madison, WI, US). In this test, a substrate (Caspase-Glo®) is used to measure caspase-3/7 activity as an apoptotic biomarker. The substrate contains the tetrapeptide DEVD (amino acid residues of glutamate-aspartate-valine-glutamate) enzymatically converted to a luminescent signal proportional to caspase-3/7. The cells (1 × 10⁴ cells/well) were seeded in 96-well plates for 24 h, and the treatments were added: Aspirin (10, 15, and 20 mM), ABJ (10, 20, and 30 %), and their combination (20 mM Aspirin + 30 % v/v ABJ). After 24 h incubation, 50 µL of Caspase-Glo® substrate were added, followed by 30 min incubation. Luminescence was measured in a plate reader (GloMax® Multi Microplate Reader, Molecular Devices, Sunnyvale, CA, US). The assay was performed in quadruplicates, and the results were expressed as relative luminescent units (RLU) compared to the negative control (cells without treatment). Cells treated with 1 % H₂O₂ (0.5 M) were used as a positive control.

2.3.5. Human apoptosis proteome analysis on cell lysates and bioinformatic analysis

The cells (1 × 10⁷ cells/well) were seeded in 96 well-plates for 24 h. Then, the cells were treated with 20 mM Aspirin, 30 % ABJ, or their combination, for 24 h. The cells were lysed with Halt™ Protease inhibitor (Thermo Fisher Scientific, Waltham, MA, US) (190 µL of protease inhibitor dissolved in 9.81 mL of PBS 1×) for 30 min at 4 °C. The total protein was quantified using the Pierce™ bicinchoninic acid (BCA) Protein Assay Kit (Thermo Fisher Scientific), and the concentration was standardized for all treatments as reported by Luzardo-Ocampo et al.

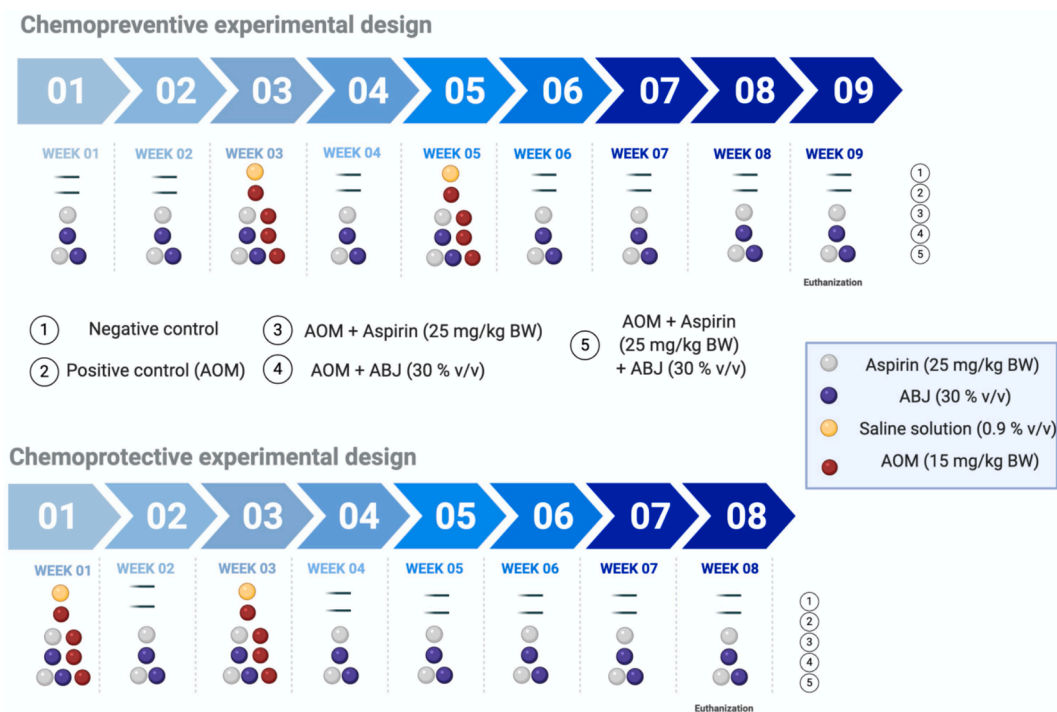


Fig. 1. *In vivo* experimental design. (A) Evaluation of the chemoprotective effect of ABJ, Aspirin, and their mixture in AOM-induced colorectal cancer Balb/c mice. (B) Evaluation of the chemopreventive effect of ABJ, Aspirin, and their mixture in AOM-induced colorectal cancer Balb/c mice. The treatments were designed to guarantee the same number of weeks from mice receiving the ABJ and Aspirin treatments. Negative control mice received two saline solution (0.9% v/v) injection. ABJ was administered in the mice drinking water *ad libitum*. All mice consumed basal diet (Rodent Lab diet) *ad libitum*. AOM was used as chemical inductor of colorectal cancer. **ABJ:** Andean berry juice; **AOM:** Azoxymethane. The graphic was done with [Biorender.com](https://biorender.com).

(2018). The obtained protein samples were analyzed following the manufacturer's instruction from the Proteome Profiler Human Apoptosis Array Kit (ARY009, R&D Systems, Minneapolis, MN, US). The relative expression of the proteins was determined in a ChemiDoc XRS⁺ Cell Imaging system (BioRad, Hercules, CA, US), and the results were quantified in the ImageLab (BioRad, US) software, being expressed as fold change against the control.

For the bioinformatics analysis, a protein interaction network, estimating the involved biological processes and interaction pathways were predicted with the STRING® platform as suggested by von Mering et al. (2007).

2.4. *In silico* analysis

An *in silico* molecular docking analysis was performed to deepen into those compounds potentially responsible for the proteomic modulation. For this, the 3D chemical structures of the potential ligands such as Aspirin (PubChem CID: 2244), gallic acid (PubChem CID: 370), chlorogenic acid (PubChem CID: 179), caffeic acid (PubChem CID: 689043), ellagic acid (PubChem CID: 5281855), *p*-coumaric acid (PubChem CID: 637542), 3,4-dihydroxybenzoic acid (PubChem CID: 72), 2-hydroxycinnamic acid (PubChem CID: 637540), (+)-catechin (PubChem CID: 9064), rutin (PubChem CID: 5280805), morin (PubChem CID: 5281670), and kaempferol (PubChem CID: 5280863) were downloaded from PubChem database (<https://pubchem.ncbi.nlm.nih.gov/>). Ligands were prepared by its conversion to.pdb files using Discovery Studio Visualizer 19.1.0.18287 (Dassault Systèmes, Vélizy-Villacoublay, France).

For the protein receptors, the 3D structures of Hsp70 (1S3X), Hsp32 (1S8C), catalase (1DGF), TRAILR1 (5CIR), Livin (1OXN), XIAP (5OQW), DIABLO (1FEW), caspase-3 subunit 12 (6BDV), caspase-3 subunit 17 (2XYP), pro-caspase-3 (4JQY), cytochrome C (3ZCF), and Bax (4BD7) were downloaded from Protein Databank website (<https://www.rcsb.org/>). For the other proteins differentially modulated by the

treatments such as p-RAD17 (O75943), CDNK1A (P38936), p27 (O43806), PON2 (ID: Q15165), HIF-1 α (Q16665), TNFRS1A (ID: P19438), TRAILR2 (O17463), clusterin (P10909), and Bad (Q92934), their FASTA sequences were downloaded from Uniprot website (<https://www.uniprot.org/>) and modeled in SwissModel 2.0 (Biasini et al., 2014) where the 3D models with the highest identities were chosen for the docking procedure (Supplementary Table S2). Water molecules and original ligands from the protein receptors were deleted using Discovery Studio Visualizer 19.1.0.18287 (Dassault Systèmes). Prepared ligands and receptors were docked, selecting flexible torsions, hydrogen bonds, and calculating docking parameters in AutoDock Vina (Trott & Olson, 2010), and following the reported procedure of Luna-Vital, Weiss, & Gonzalez de Mejia (2017). The visualization of the best docking poses was conducted using the output files from AutoDock Vina in Discovery Studio Visualizer 19.1.0.18287 (Dassault Systèmes). For the calculation of the inhibition constant values using the binding energy values, the following equation was used: $\Delta G: -RT \cdot \ln K$, where ΔG denotes the Gibbs free energy, R is the Raoult gas constant (1.986 cal/mol·K), and T is the temperature of the reaction (ideally: 298 K).

2.5. *In vivo* assays

2.5.1. Animal husbandry and treatments

This project was approved by the Ethics Committee for Animal Experimentation from University of Antioquia (approval code: 125 from June 4, 2019). The animal experiments were carried out according to national (Law 84/1989, Resolution 8430/1993) and international (National Institute of Health, NIH) guidelines. Male and female Balb/c (8 weeks age, 16–25 g initial body weight, BW) were maintained at 22–25 °C and 12 h/12 h light/dark cycle at the PECET-SIU Laboratory Animal Facility from University of Antioquia. The animals were fed with a standard rodent diet (basal diet, BD, LabDiet 5010) and maintained in plastic cages (6 animals/cage, n = 30 animals).

After 1-week acclimatization, the mice were randomly assigned to 6

Table 1Experimental design followed for the *in vivo* assessment.

Week	Negative Control	Positive control	AOM + Aspirin	AOM + ABJ	AOM + Aspirin + ABJ
<i>Chemopreventive Administration</i>					
1	–	–	Aspirin	ABJ	Aspirin + ABJ
2	–	–	Aspirin	ABJ	Aspirin + ABJ
3	Saline solution	AOM	AOM + Aspirin	AOM + ABJ	AOM + Aspirin + ABJ
4	–	–	Aspirin	ABJ	Aspirin + ABJ
5	Saline solution	AOM	AOM + Aspirin	AOM + ABJ	AOM + Aspirin + ABJ
6	–	–	Aspirin	ABJ	Aspirin + ABJ
7	–	–	Aspirin	ABJ	Aspirin + ABJ
8	–	–	Aspirin	ABJ	Aspirin + ABJ
9	–	–	Aspirin	ABJ	Aspirin + ABJ
<i>Chemoprotective Administration</i>					
1	Saline solution	AOM	AOM + Aspirin	AOM + ABJ	AOM + Aspirin + ABJ
2	–	–	Aspirin	ABJ	Aspirin + ABJ
3	Saline solution	AOM	AOM + Aspirin	AOM + ABJ	AOM + Aspirin + ABJ
4	–	–	Aspirin	ABJ	Aspirin + ABJ
5	–	–	Aspirin	ABJ	Aspirin + ABJ
6	–	–	Aspirin	ABJ	Aspirin + ABJ
7	–	–	Aspirin	ABJ	Aspirin + ABJ
8	–	–	Aspirin	ABJ	Aspirin + ABJ

ABJ: Andean berry (*V. meridionale* Sw.) juice (30 % v/v); **AOM:** Azoxymethane (15 mg/kg body weight, BW). Aspirin was administered in a 25 mg/kg BW concentration. The saline solution was at 0.9 % w/v concentration.

experimental groups (n = 6 mice/group) as follows: negative control (intraperitoneal injection – i. p.- of 10 mg/kg BW 0.9 % v/v saline physiological solution), positive control (azoxymethane or AOM, i. p. of 15 mg/kg BW), AOM + Aspirin (AOM: 15 mg/kg BW + 20 mM Aspirin), AOM + ABJ (AOM: 15 mg/kg BW + 30 % v/v ABJ), AOM + Aspirin + ABJ (AOM: 15 mg/kg BW + 20 mM Aspirin + 30 % ABJ). Two randomized block experimental designs were followed: chemoprotective and chemopreventive. For the chemoprotective evaluation of ABJ and Aspirin, colorectal cancer was induced while the treatments' administration (total experiment: 8 weeks). For the chemopreventive evaluation of ABJ and Aspirin, the treatments were administered two weeks before inducing colorectal cancer with AOM (9 weeks of the total experiment). A diagram of both approaches is shown in Fig. 1 and Table 1. All mice were fed with water and basal diet *ad libitum*. The treatments (ABJ and Aspirin) were dissolved in the mice's drinking water and filtered (0.45 µm filters).

2.5.2. Macroscopic measurements

2.5.2.1. Body and relative organs' weight. Body weight was measured weekly during the experimental procedure. At the end of the experiments, animals were anesthetized, euthanized, and dissected. All livers and colon were excised, and their weight was normalized against the mice's weight.

2.5.2.2. Aberrant crypt foci (ACF) analysis. Once euthanized, the colon was excised, weighed, and prepared for ACF analysis, as reported by Raju (2008). Briefly, 4 cm of the distal section was washed with physiological saline solution (0.9 % v/v), longitudinally opened, and fixed with 10 % buffered formalin solution. The samples were stained with 0.2 % methylene blue, and then washed with Krebs-Ringer buffer solution [118 mM NaCl, 4.7 KCl, 1.2 mM MgSO₄, 1.2 mM KH₂PO₄, 25 mM NaHCO₃, 11 mM glucose, and 2.5 mM CaCl₂; pH: 6.8]. Readings were carried out in an inverted microscope at 10 × to identify the presence, quantity, and multiplicity of ACF. The ACF were defined as those with the biggest size, thickened edges, and a higher pericrypt space than normal crypts. The multiplicity was considered as the number of crypts

by foci. Results were reported in number of ACF.

2.5.3. Histopathologic analysis

Samples of the colon, liver, and spleen were used for the histopathological analysis. Tissues were fixed in 10 % buffered formalin solution for at least 24 h. Then, alcohol-series dehydration was conducted, and the obtained tissues were embedded in paraffin to be sectioned in 5 µm slides using a microtome (Luzardo-Ocampo et al., 2020a). The sections were stained with hematoxylin and eosin (H&E). The liver evaluations were conducted since this organ is critical for the metabolic activation of AOM and shows physical changes due to AOM treatment (Suzuki et al., 2006).

2.6. Statistical analysis

Unless indicated, all results were expressed as mean ± standard deviation (SD) from three independent experiments in triplicates. For the *in vitro* tests, a one-way ANOVA analysis was conducted, followed by a *post-hoc* Tukey-Kramer analysis. For the *in vivo* tests, one-way ANOVA was carried out, followed by a *post-hoc* Kruskal-Wallis test. The data normality was assessed by analyzing the data's normal distribution, normal quantile plots, and the Shapiro-Wilk test. The statistical analysis was set at *p* < 0.05. The JMP software v. 14.0 (SAS Institute, USA) was used for the analyses, and GraphPad Prism v. 8.0 was used to calculate half-inhibitory concentrations (IC₅₀) from *in vitro* tests.

3. Results

3.1. ABJ polyphenolic composition

Seven phenolic acids and four flavonoids were identified in ABJ by HPLC-DAD, where 3,4-dihydroxybenzoic and gallic acids are the most abundant phenolic acids (Supplementary Table S3). For the flavonoids, rutin and morin showed the highest content. As these were the primary identified phenolic compounds in ABJ, the subsequent *in silico* analysis was conducted between these potential ligands and selected protein targets evaluated in this research. It is important to clarify that these compounds were found as the most abundant in ABJ, but other phenolic compounds could not be identified since additional HPLC standards were not tested.

3.2. Aspirin, ABJ, and their mixture decreased SW480 cell viability

Fig. 2 shows the antiproliferative assessment for all the treatments. Aspirin concentrations ≥ 10 % v/v showed SW480 cell viabilities < 80 % at 24, 48, and 72 h of treatment, being the 72 h treatments the most effective. This could be confirmed by the IC₅₀ values, where 24 h (Fig. 2B) and 48 h (Fig. 2C) almost remained the same, while 72 h (Fig. 2D) was the lowest (–21.70 % for both 24 h and 48 h). Similar behavior was shown for ABJ, where ABJ concentrations ≥ 10 % v/v also displayed the same effect on cell viability at 24–72 h treatments. However, as long the treatment was applied, the lowest the IC₅₀: 24 h (Fig. 2F) > 48 h (Fig. 2E) > 72 h (Fig. 2F). The Aspirin (20 mM) and ABJ (30 % v/v) mixture showed a higher decrease in cell viability, as shown in Fig. 2I. These concentrations of Aspirin and ABJ were selected as both were the most effective in reducing the viability in the previous tests. Considering the polyphenolic composition of ABJ (Supplementary Table S3), the IC₅₀ 72 h is equivalent to 91.12 ± 1.22 µg/g gallic acid, 4.89 ± 0.40 µg/g chlorogenic acid, 1.59 ± 0.01 µg/g caffeic acid, 9.59 ± 0.69 µg/g ellagic acid, 0.90 ± 0.03 µg/g *p*-coumaric acid, 112.00 ± 0.12 µg/g 3,4-dihydroxybenzoic acid, 0.05 ± 0.00 µg/g 2-hydroxycinnamic acid, 5.72 ± 0.01 µg/g (+)-catechin, 15.39 ± 0.04 µg/g rutin, 18.53 ± 1.07 µg/g morin, and 2.02 ± 0.01 µg/g kaempferol.

To evaluate the ability of SW480 cells to proliferate, the cloning efficiency test was conducted. Representative pictures are shown in Fig. 2J, indicating that none of the cells could proliferate at the assessed

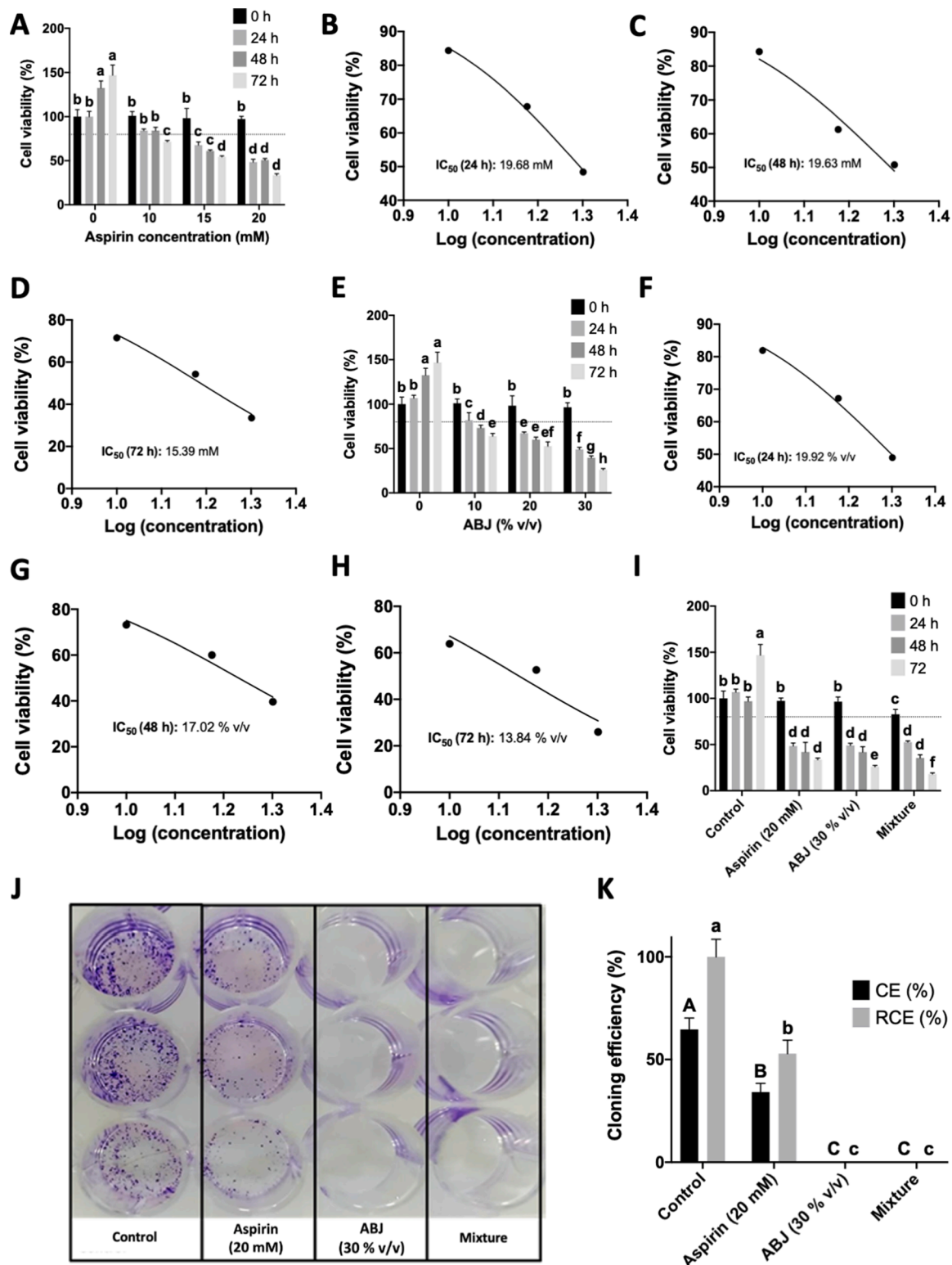


Fig. 2. Effect of Aspirin, ABJ, and their mixture on the SW480 cell viability and cloning efficiency. Impact of Aspirin on the (A) cell viability and calculated IC₅₀ at (B) 24 h, (C) 48 h and (D) 72 h. Influence of ABJ treatments on the (E) cell viability calculated IC₅₀ at (F) 24 h, (G) 48 h and (H) 72 h. (E) Assessment of the Aspirin (20 mM) and ABJ (30 % v/v) mixture on the cell viability. (F) Representative pictures from positive stained cells with Carnoy's solution after the assayed treatments and (G) cloning efficiency (CE, %) and (G). relative CE (RCE) quantification (%). For the bar graphics (1A and 1I), the results were expressed as mean ± SD of three independent experiments in triplicates. Different letters express significant differences ($p < 0.01$) by Tukey-Kramer's test. The dotted line shows 80 % cell viability. The obtained ANOVA p-values for the figures were $p = 0.0089$ (Fig. 1A), $p = 0.0078$ (Fig. 1B), and $p = 0.0086$ (Fig. 1I). For the cloning efficiency (1 K), upper-case and lower-case letters indicate significant differences ($p < 0.05$) between CE and RCE values, respectively, by Tukey-Kramer's test. The obtained ANOVA p-value for the Fig. 1K was $p = 0.0345$. The half inhibitory concentrations (IC₅₀) were calculated using a biological-adjusted equation from GraphPad Prism v. 8.0. For all the experiments, the control corresponded to untreated (ITS medium only) SW480 cells. The mixture corresponded to Aspirin (20 mM) + ABJ (30 % v/v). **ABJ:** Andean berry juice.

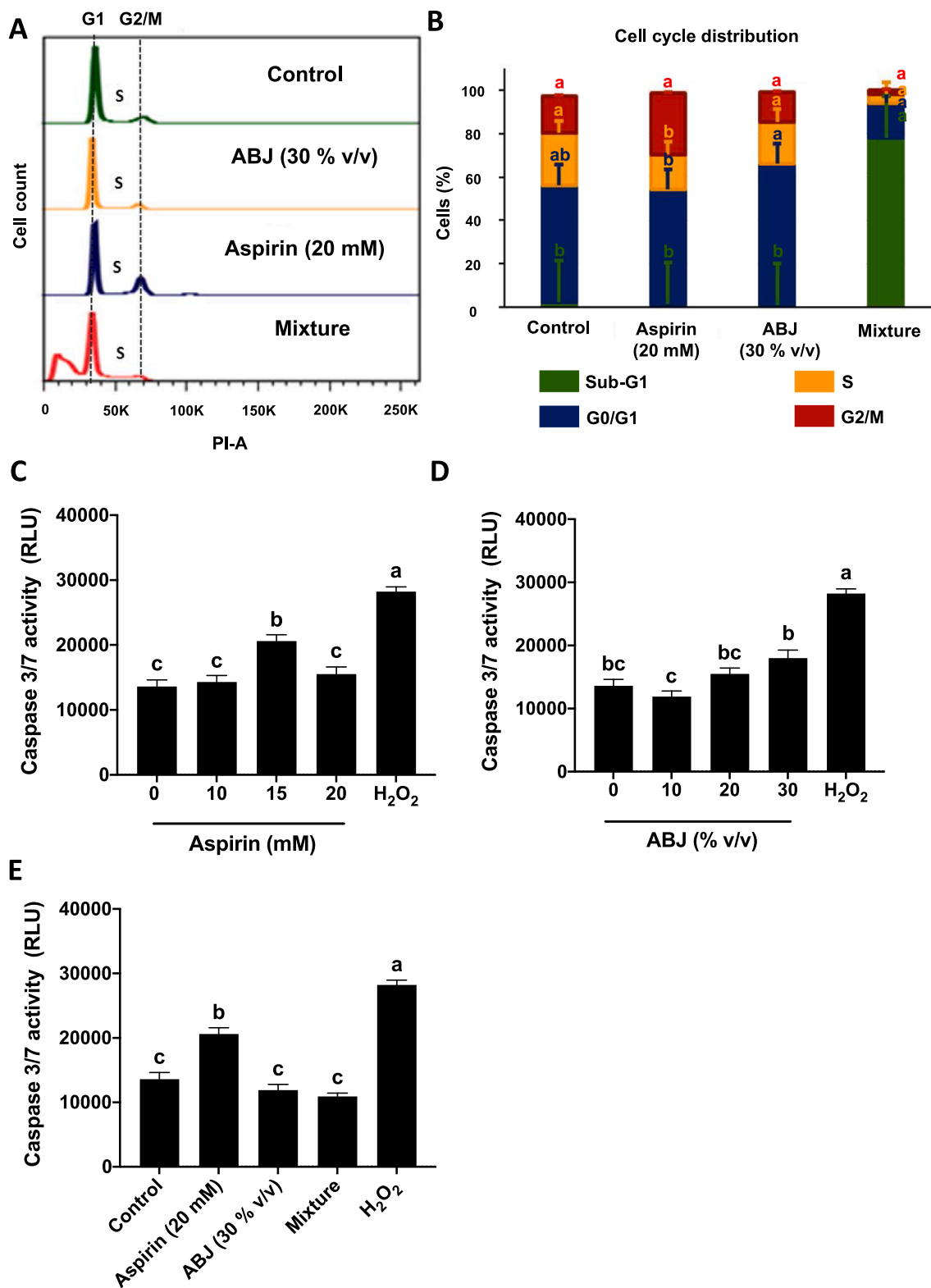


Fig. 3. Impact of Aspirin, ABJ, and their mixture on the SW480 cell cycle distribution and Caspase-3/7 activity. (A) Representative pictures from the IP intensity histograms and (B) percentage of SW480 cells on each cell cycle's stage. Caspase-3/7 activity after treatment with (C) Aspirin, (D) ABJ, and (E) their mixture. Results from the bar graphics (2B, 2C, 2D, and 2E) are the mean ± SD of three independent experiments in triplicates. For the cell cycle distribution (2A), different letters indicate significant differences ($p < 0.05$) between treatments and for the same cell cycle's phase. The obtained ANOVA p-value for the figure was $p = 0.0477$. For the Caspase-3/7 activity (2C, 2D, and 2E) different letters express significant differences ($p < 0.01$) between treatments by Tukey-Kramer's test. The obtained ANOVA p-value for the figures were $p = 0.0087$ (2C), $p = 0.0076$ (2D), and $p = 0.0081$ (2E). For all the experiments, the control corresponded to untreated (ITS medium only) SW480 cells. Hydrogen peroxide (H₂O₂, 0.5 M) was used as the positive control. The mixture corresponded to Aspirin (20 mM) + ABJ (30 % v/v). **ABJ:** Andean berry juice; **PI-A:** Propidium Iodide-Annexin V; **RLU:** Relative Luminescence Units.

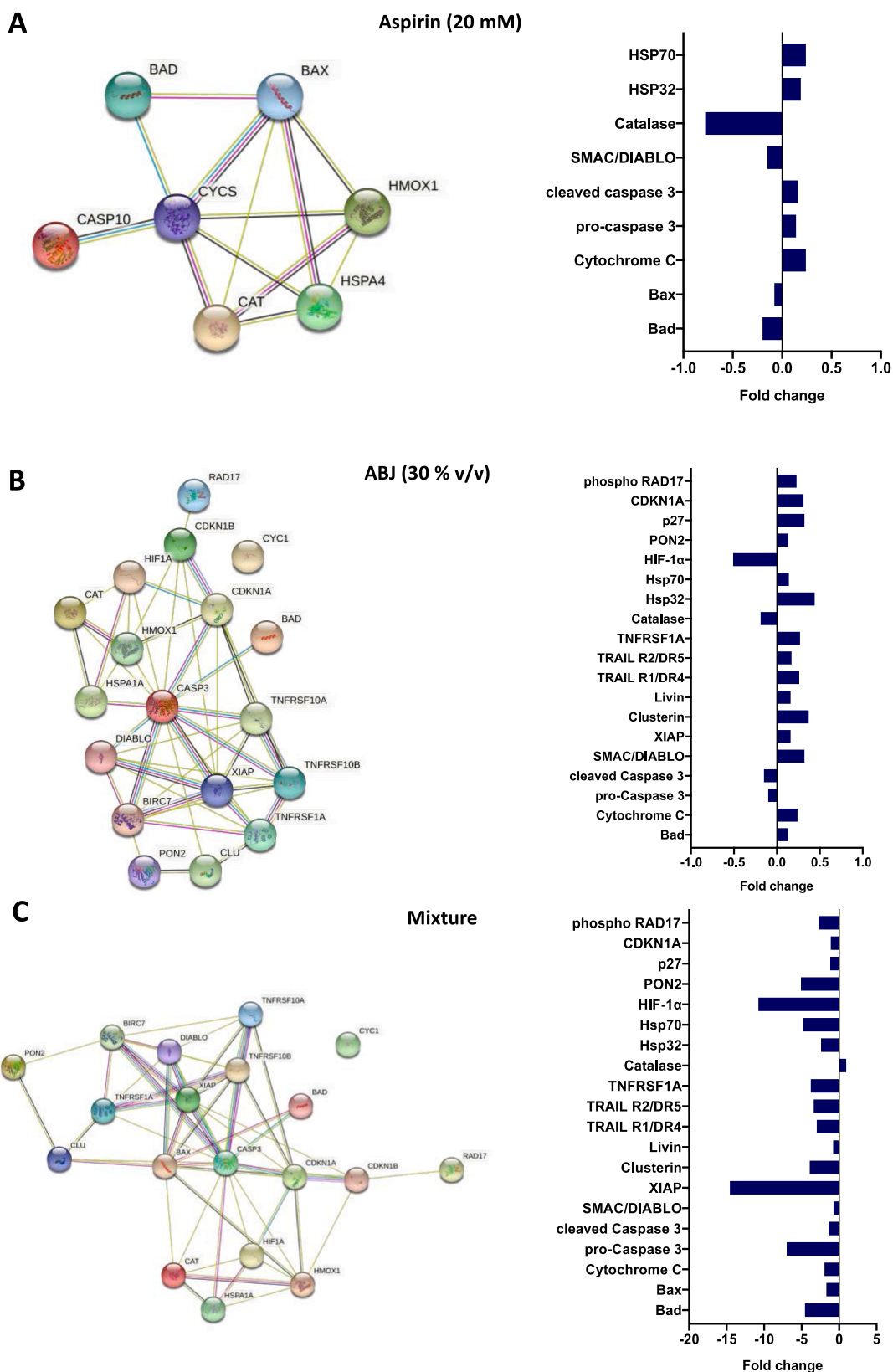


Fig. 4. Assessment of the effect of Aspirin, ABJ, and their mixture on the modulation of apoptotic proteins in SW480 cells. Representative protein STRING® network and fold-change against the control for (A) Aspirin, (B) ABJ, and (C) their mixture. Aspirin (20 mM), ABJ (30 % v/v), and their mixture (20 mM Aspirin + 30 % v/v ABJ) were used as treatments for SW480 cells. The control corresponded to untreated (ITS medium only) SW480 cells. Treatments were applied for 24 h after cell confluence.

Table 2

Molecular function (gene ontology) involved biological processes, and KEGG pathways after the STRING® analysis of apoptosis-modulation by Aspirin, ABJ, and their mixture.

Aspirin		ABJ		Mixture (ABJ + Aspirin)	
Molecular function (GO)	FDR	Molecular function (GO)	FDR	Molecular function (GO)	FDR
Cysteine-type endopeptidase activator activity involved in apoptotic process	2.00 × 10 ⁻³	Cysteine-type endopeptidase regulator activity involved in apoptotic process	1.61 × 10 ⁻⁵	Cysteine-type endopeptidase regulator activity involved in apoptotic process	2.11 × 10 ⁻⁵
Heme binding	2.00 × 10 ⁻³	Cyclin-dependent protein serine/threonine kinase inhibitor activity	2.72 × 10 ⁻⁵	Cyclin-dependent protein serine/threonine kinase inhibitor activity	3.36 × 10 ⁻⁵
Enzyme binding	1.33 × 10 ⁻³	Enzyme binding	3.37 × 10 ⁻⁵	Enzyme binding	7.44 × 10 ⁻⁵
Heat shock protein binding	1.33 × 10 ⁻³	TNF-receptor activity	9.74 × 10 ⁻⁵	TNF-receptor activity	1.20 × 10 ⁻⁴
Cofactor binding	1.33 × 10 ⁻³	TRAIL binding	3.90 × 10 ⁻⁴	Heat shock protein binding	1.40 × 10 ⁻⁴
Protein dimerization activity	1.37 × 10 ⁻³	Enzyme-inhibitor activity	4.50 × 10 ⁻⁴	Protein binding	1.90 × 10 ⁻⁴
Oxidoreductase activity	2.71 × 10 ⁻³	Protein-binding	4.50 × 10 ⁻⁴	TRAIL binding	3.60 × 10 ⁻⁴
Biological Process	FDR	Biological Process	FDR	Biological Process	FDR
Intrinsic apoptotic signaling pathway	2.76 × 10 ⁻⁶	Regulation of apoptotic process	2.23 × 10 ⁻¹¹	Regulation of apoptotic process	2.24 × 10 ⁻¹²
Activation of cysteine-type endopeptidase activity involved in apoptotic process	1.84 × 10 ⁻⁵	Negative regulation of programmed cell death	2.23 × 10 ⁻¹¹	Negative regulation of programmed cell death	2.24 × 10 ⁻¹²
Extrinsic apoptotic signaling pathway	2.15 × 10 ⁻⁵	Neg. regulation of apoptotic process	2.29 × 10 ⁻¹⁰	Intrinsic apoptotic signaling pathway	5.09 × 10 ⁻¹²
Response to hydrogen peroxide	2.18 × 10 ⁻⁵	Intrinsic apoptotic signaling pathway	2.29 × 10 ⁻¹⁰	Negative regulation of apoptotic process	1.39 × 10 ⁻¹¹
Positive regulation of proteolysis	2.21 × 10 ⁻⁵	Apoptotic signaling pathway	4.25 × 10 ⁻¹⁰	Apoptotic signaling pathway	1.39 × 10 ⁻¹¹
Response to oxidative stress	2.21 × 10 ⁻⁵	Programmed cell death	1.44 × 10 ⁻⁹	Programmed cell death	1.24 × 10 ⁻¹⁰
Regulation of apoptotic process	2.32 × 10 ⁻⁵	Cellular response to stress	4.71 × 10 ⁻⁹	Extrinsic apoptotic signaling pathway via death domain receptors	1.74 × 10 ⁻¹⁰
KEGG Pathways	FDR	KEGG Pathways	FDR	KEGG Pathways	FDR
Apoptosis	7.42 × 10 ⁻⁶	Apoptosis	2.92 × 10 ⁻⁹	Apoptosis	5.10 × 10 ⁻¹¹
Apoptosis – Multiple species	7.91 × 10 ⁻⁶	Apoptosis – Multiple species	7.15 × 10 ⁻⁹	Apoptosis – Multiple species	5.10 × 10 ⁻¹¹

Table 2 (continued)

Aspirin		ABJ		Mixture (ABJ + Aspirin)	
Molecular function (GO)	FDR	Molecular function (GO)	FDR	Molecular function (GO)	FDR
Platinum drug resistance	6.12 × 10 ⁻⁵	Pathways in cancer	2.29 × 10 ⁻⁷	Pathways in cancer	1.26 × 10 ⁻⁸
Colorectal cancer	8.61 × 10 ⁻⁵	Platinum drug resistance	8.52 × 10 ⁻⁶	Platinum drug resistance	1.25 × 10 ⁻⁷
Pathways in cancer	3.10 × 10 ⁻⁴	HIF-1 signaling pathway	2.71 × 10 ⁻⁵	Necroptosis	4.39 × 10 ⁻⁶
p53 signaling pathway	1.50 × 10 ⁻³	MicroRNAs in cancer	9.06 × 10 ⁻⁵	p53 signaling pathway	6.18 × 10 ⁻⁶

ABJ: Andean berry (*Vaccinium meridionale* Swartz) juice; FDR: False discovery rate; GO: Gene ontology; HIF: Hypoxia-inducible factor; KEGG: Kyoto encyclopedia of genes and genomes; TNF: Tumor necrosis factor; TRAIL: TNF-related apoptosis-inducing ligand.

ABJ (30 % v/v) concentration nor its mixture with Aspirin, despite that some of them could proliferate with Aspirin (20 mM). The quantification of CE and RCE percentages (Fig. 2K) was in line with the plate observations.

3.3. Impact of ABJ, Aspirin, and their mixture on the cell cycle distribution and caspase-3/7 activity of SW480 cells

The influence of the treatments on the cell cycle distribution is shown in the representative histogram pictures for all the treatments (Fig. 3A) and their quantification (Fig. 3B). Compared to the untreated control, Aspirin-treated cells exhibited a decrease ($p > 0.01$) in the S-subpopulation was observed (−13.50 %) and an increase ($p < 0.01$) in the G2/M-subpopulation (+22.70 %). ABJ displayed a 65.7 % increase in the G0/G1 subpopulation ($p > 0.01$) and a 17.10 % decrease in the G2/M subpopulation ($p < 0.01$) when compared to the untreated control cells, suggesting a cell cycle arrest. The ABJ + Aspirin mixture showed a 78.3 % increase in the subG1 phase and a reduction in all the other phases (G0/G1, S, and G2/M) ($p < 0.01$) compared to the untreated control.

For the caspase-3/7 activity, all Aspirin concentrations decreased the activity, but none of the treatments were different from those of the untreated cells (Fig. 3C). Regarding ABJ (Fig. 3D), only 10 % v/v showed a lower activity, exhibiting the same outcomes as Aspirin + ABJ (30 % v/v) mixture, suggesting a synergistic activity between both. These results showed that apoptosis is not the main ABJ-induced cell death mechanism induced. As observed in the subsequent analyses, mechanisms associated with HIF-1 α , necroptosis, or the activation of specific receptors are potentially modulated by ABJ.

3.4. Effect of Aspirin, ABJ, and their mixture in the modulation of pro-apoptotic proteins in SW480 cells

Fig. 4 shows the proteomic analysis of pro-apoptotic proteins in SW480 after being treated with 20 mM Aspirin. The protein arrangement of Aspirin was predicted by STRING® based on the fold-changes values obtained from protein expression of treated SW480 cells against the untreated cells (Fig. 4A), being catalase and DIABLO the proteins with the lowest expression, and Cytochrome C and Hsp70 those with the highest expression. Both ABJ (30 % v/v) (Fig. 4B) and the mixture (Fig. 4C) showed the highest number of modulated proteins (19 and 30, respectively). Compared to the mixture, ABJ mainly exhibited an increase in the expression of all the modulated protein except by hypoxia-inducible factor 1 α (HIF-1 α : fold change: −0.51), catalase (fold change: −0.19), and cleaved caspase-3 (fold change: −0.15) (Fig. 4B). The positively regulated proteins showed the highest values: heat-shock

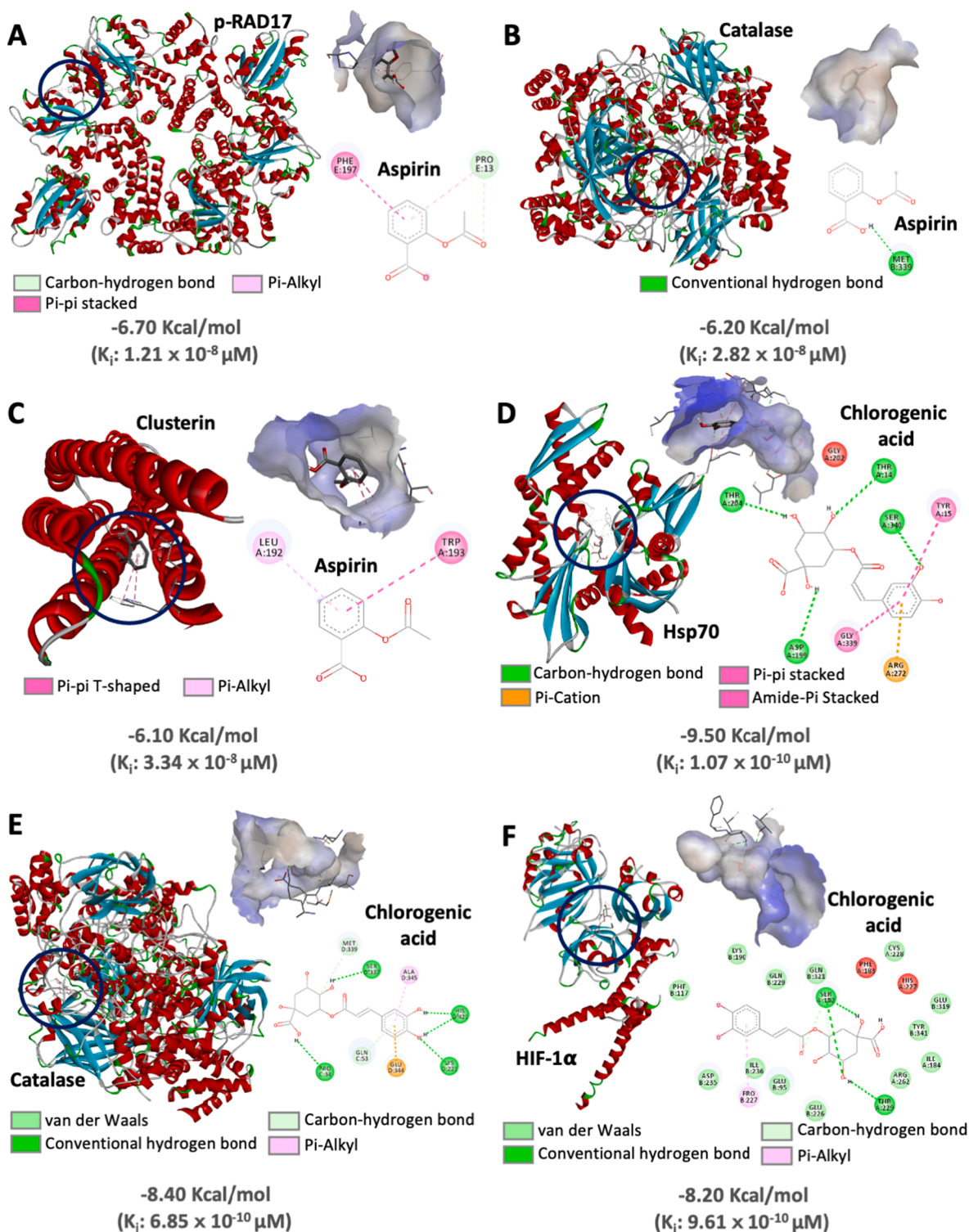


Fig. 5. *In silico* analysis between selected treatments and target proteins from the apoptosis modulation in SW480 cells. Best docking binding between Aspirin and (A) p-RAD17, (B) Catalase, and (C) Clusterin. Best docking binding between Chlorogenic acid and (D) Hsp70, (E) Catalase, and (F) HIF-1 α . The graphic represents the overall protein receptor-ligand interaction (blue circle), the specific protein receptor-ligand interaction, and the 2D representation of the involved amino acids in the interaction. The gray values indicate the binding energy in kcal/mol. The calculated inhibition constant (K_i) for each interaction is also shown in μM . (For interpretation of the references to color in this figure legend, the reader is referred to the web version of this article.)

protein 32 (Hsp32, fold change: 0.44) and Clusterin (fold change: 0.37). The mixture exhibited the largest fold-change values (Fig. 4C), being XIAP (X-linked inhibitor of apoptosis, fold change: -14.57), HIF-1 α (fold change: -10.78), and pro-caspase 3 (fold change: -6.98) the highest values.

The bioinformatics analysis of the main molecular functions, biological processes, and Kyoto Encyclopedia of Genes and Genomes (KEGG) pathways is presented in Table 2. As observed, all treatments showed similar molecular functions, but treatments including ABJ predicted TNF-receptor activity and TRAIL binding, suggesting an ABJ

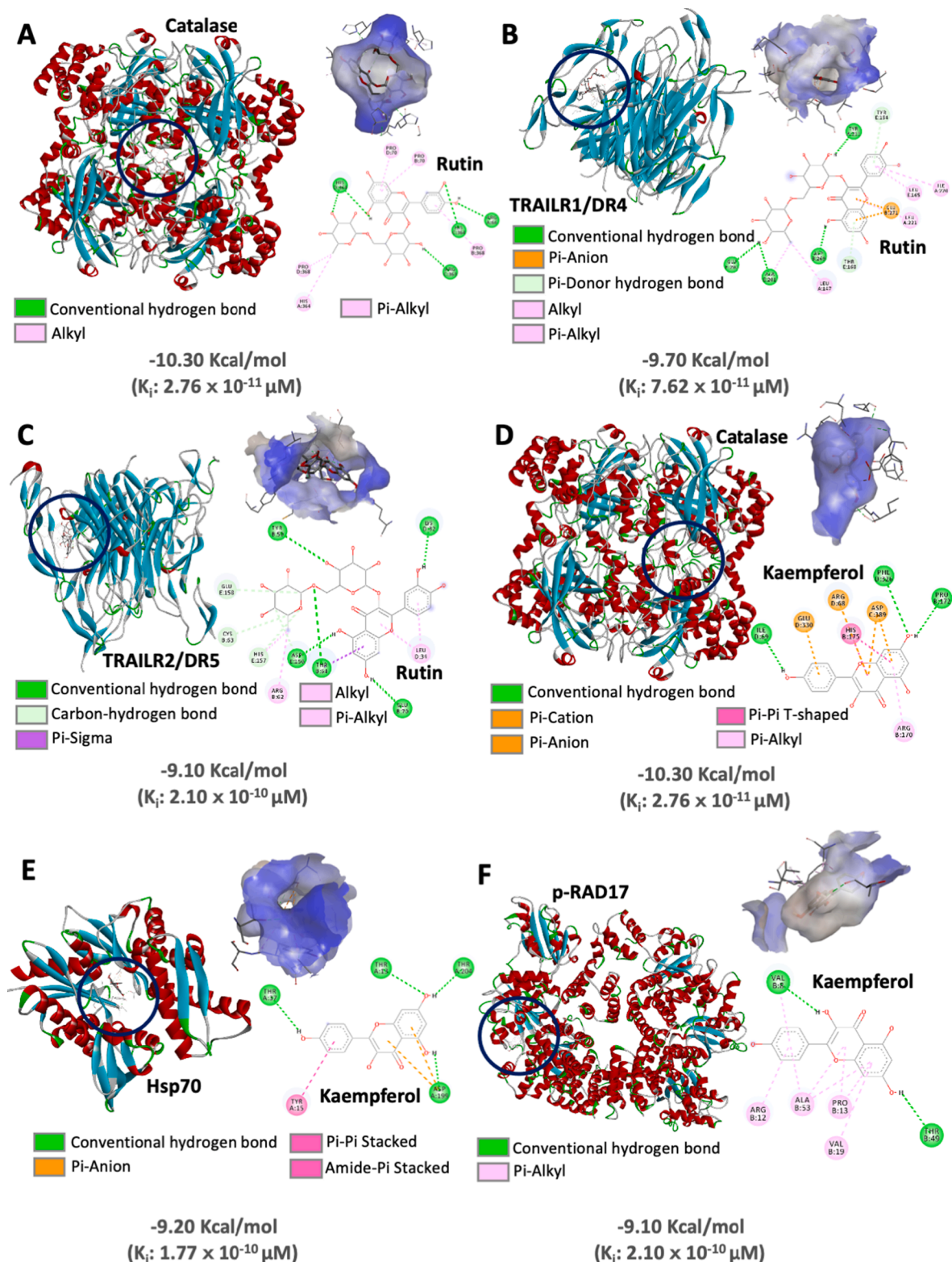


Fig. 6. *In silico* analysis between selected treatments and target proteins from the apoptosis modulation in SW480 cells. Best docking binding between rutin and (A) Catalase, (B) TRAILR1/DR4, and (C) TRAILR2/DR5. Best docking binding between Kaempferol and (D) Catalase, (E) Hsp70, and (F) p-RAD17. The graphic represents the overall protein receptor-ligand interaction (blue circle), the specific protein receptor-ligand interaction, and the 2D representation of the involved amino acids in the interaction. The calculated inhibition constant (K_i) for each interaction is also shown in μM . (For interpretation of the references to color in this figure legend, the reader is referred to the web version of this article.)

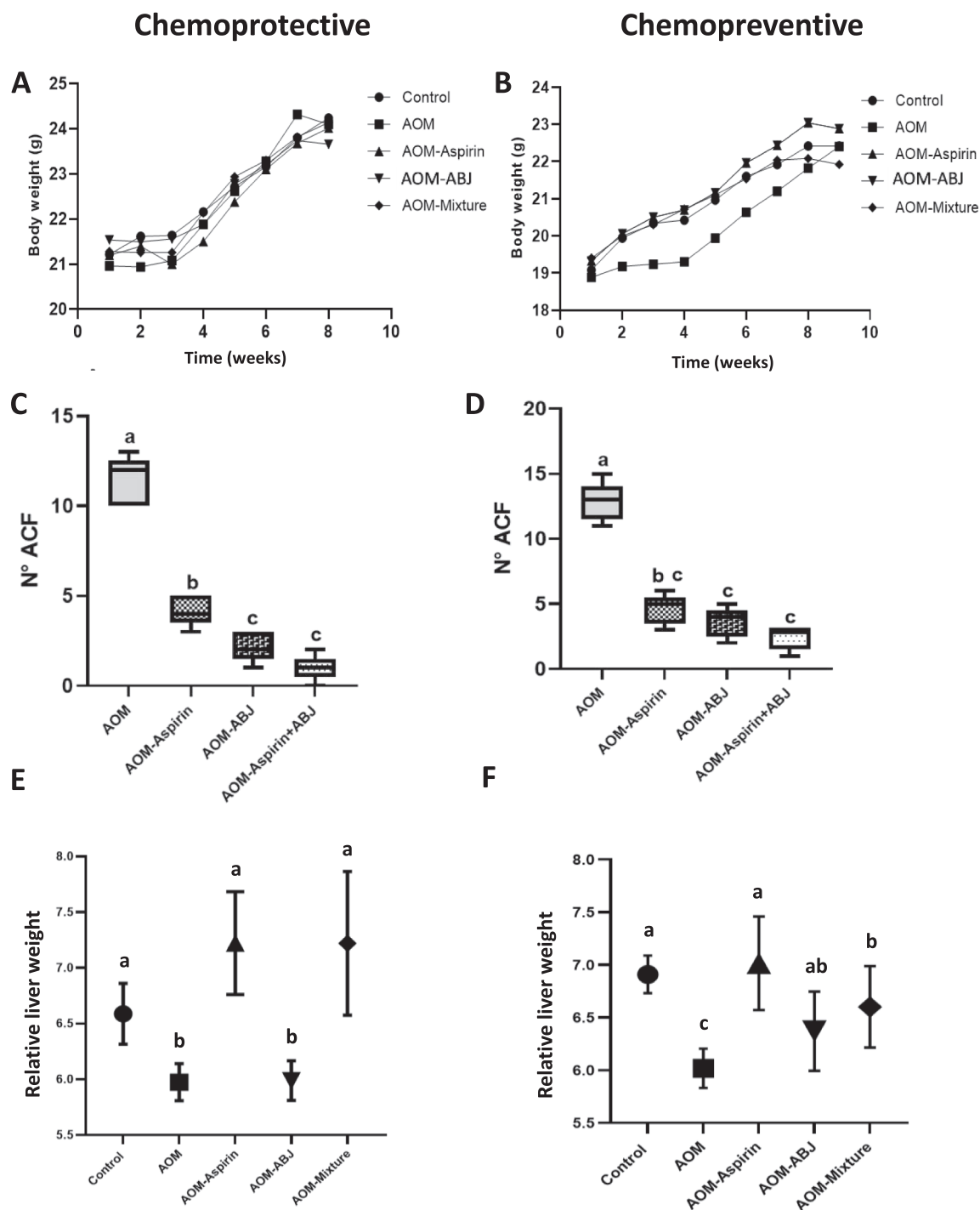


Fig. 7. Impact of the treatments on the chemoprotective and chemopreventive evaluation of colorectal cancer *in vivo*. (A) Body weight during chemoprotective evaluation; (B) Body weight evolution during chemopreventive evaluation; (C) Number of aberrant crypt foci (ACF) during chemoprotective evaluation; (D) Number of ACF during chemopreventive evaluation; (E) Relative liver weight during chemoprotective evaluation; (F) Relative liver weight during chemopreventive evaluation. The results were expressed as mean \pm SD of six animals. The letters express significant differences ($p < 0.05$) by Kruskal-Wallis test. The obtained p-values for the figures were $p = 0.0665$ (Fig. 7A), $p = 0.0634$ (Fig. 7B), $p = 0.0299$ (Fig. 7C), $p = 0.0430$ (Fig. 7D), $p = 0.045$ (Fig. 7E), and $p = 0.034$ (Fig. 7F). There were no differences for body weight during the treatments. **ABJ**: Andean berry juice; **ACF**: Aberrant Crypt Foci; **AOM**: Azoxy methane (15 mg/kg BW). The control corresponded to untreated mice. All mice consumed basal diet *ad libitum*.

preference by extrinsic apoptotic processes. Most biological processes were associated with the negative regulation of cell death, the apoptotic signaling pathway, and cell response to stress. Apoptosis is the main developed process by all treatments, as predicted by the KEGG pathways, but Aspirin showed a predicted p53 activation, whereas ABJ treatments indicated HIF-1 α mechanism (ABJ) and necroptosis (ABJ +

Aspirin).

3.5. Assessment of the *in silico* binding affinity of Aspirin and ABJ phenolic compounds with selected Apoptotic-related protein targets

To deepen the potential interaction with Aspirin and some ABJ

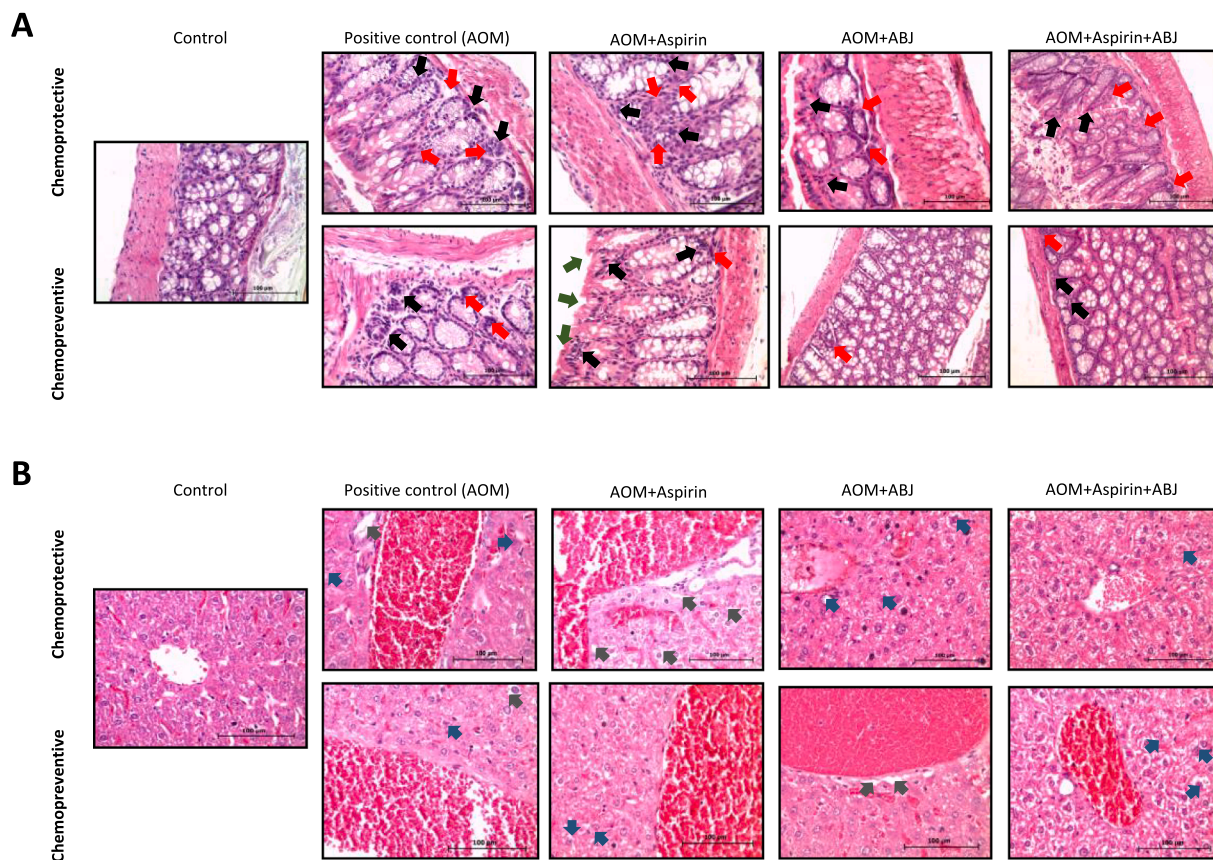


Fig. 8. Representative pictures from the histopathologic analysis of (A) colon and (B) liver tissues excised from Balb/c mice at the end of the experimental procedure. For the colon (A), black arrows: indicate immune cell infiltration; red arrows: loss of colonic architecture; green arrows: epithelial erosion. For the liver (B), gray arrows: lipid accumulation (steatosis); blue arrow: loss of hepatocyte morphology. ABJ: Andean berry juice; AOM: Azoxymethane (15 mg/kg body weight). All pictures were taken at 100 × and tissues were stained with hematoxylin and eosin (H&E). (For interpretation of the references to color in this figure legend, the reader is referred to the web version of this article.)

phenolic compounds with selected apoptotic-related protein targets, an *in silico* analysis was conducted, selecting the highest binding affinities. After performing all the potential combinations between Aspirin, ABJ's phenolic compounds, and all the modulated proteins from the Human Apoptosis Array analyzed by STRING®, the lowest binding energies (Supplementary Table S4) were selected to be graphed. Fig. 5 shows the interactions between Aspirin and p-RAD17 (Fig. 5A), catalase (Fig. 5B), and clusterin (Fig. 5C). Moreover, the interactions between a phenolic acid from ABJ, chlorogenic acid, and Hsp70 (Fig. 5D), catalase (Fig. 5E), and HIF-1 α (Fig. 5F) are also shown. Most binding energies from Aspirin were considered medium (between -4.70 and -6.20 Kcal/mol), and clusterin displayed the lowest value. Aspirin interaction with catalase showed was the only one showing conventional hydrogen bond among all Aspirin evaluations, while Aspirin-p-RAD 17 was unique displaying carbon-hydrogen bond. For chlorogenic acid, interactions with Hsp70 showed the lowest binding energy (Fig. 5D). In contrast, catalase, and HIF-1 α binding energy were similar, despite that chlorogenic acid vs. HIF-1 α exhibits the highest amount of amino acid interactions (16) but showed two unfavorable interactions (red-colored amino acids) at phenylalanine 183 and histidine 227 from HIF-1 α , which could potentially explain why its binding energy is lower than the other two interactions. The calculated inhibition constants for all the assayed compounds are shown in Supplementary Table S5, whereas the amino acid interactions can be visualized more specifically at Supplementary Table S6.

Fig. 6 shows the interactions between rutin and catalase (Fig. 6A), the tumor necrosis factor (TNF)-related apoptosis-inducing ligand receptor 1 (TRAILR1) (Fig. 6B), and TRAIL receptor 2 (TRAILR2) (Fig. 6C).

Another ABJ flavonoid that showed some of the lowest binding energies was kaempferol, interacting with catalase (Fig. 6D), Hsp70 (Fig. 6E), and p-RAD17 (Fig. 6F). The rutin-catalase interaction (Fig. 6A) displayed the lowest binding energy (-10.30 Kcal/mol) and the lowest amount of amino acid interactions (9) among all rutin *in silico* assays. Despite being structurally similar, TRAILR1 showed a lowest binding energy than TRAILR2, but both shared similar amino acid interactions, such as Alkyl and Pi-Alkyl. The lowest binding energy of kaempferol was the same as the best rutin docking (Fig. 5D), while the other kaempferol interactions also showed similar values. It is important to note that *in silico* studies are limited indicating the binding affinity of the bioactive compounds of ABJ or Aspirin with selected cancer targets, but additional experiments demonstrating inhibition or activation of these molecules are required.

3.6. Evaluation of Aspirin, ABJ, and their mixture on the body weight, ACF, and relative liver weight on chemopreventive and chemoprotective AOM-induced CRC

There were no significant changes ($p < 0.01$) in the bodyweight of untreated and AOM-treated Balb/c mice in both chemoprotective (Fig. 7A) and chemopreventive (Fig. 7B) approaches. The evaluation of ACF post-euthanization showed that all the treatments were successfully decreasing ACF, displayed a similar amount in the chemoprotective (Fig. 7C) and chemopreventive (Fig. 7D) evaluation. However, AOM-treated mice from the chemopreventive evaluation developed more ACF than their counterparts from the chemoprotective approach. Surprisingly, AOM and AOM-ABJ displayed the lowest values regarding the

relative liver weight, while the untreated control and Aspirin/Mixture treated mice exhibited the highest relative weight in the chemoprotective approach (Fig. 7E). Similarly, untreated mice (control) and AOM-Aspirin were the highest values, but AOM was the lowest in the chemopreventive evaluation (Fig. 7F). None of the experimental approaches displayed significant differences between the treatments for the relative colon weight (Supplementary Fig. S1).

3.7. Colon and liver histopathologic analyses

Fig. 8 shows the representative H&E-stained pictures of the colon (Fig. 8A) and liver (Fig. 8B) from Balb/c mice under all the chemoprotective and chemopreventive approaches. Intestinal tissues of AOM-mice from the chemoprotective evaluations showed higher damage induced by the AOM treatment, such as cell infiltration (black arrows), loss of colonic architecture and potential crypt fusion (red arrows), and external epithelial erosion (green arrows). The control (untreated mice) did not show any damage, while ABJ and the mixture exhibited the best protective effects against AOM in chemopreventive and chemoprotective evaluations. Control liver tissues (Fig. 8B) did not show any damage, while those from AOM-treated mice exhibited loss of hepatocyte morphology (blue arrows) and potential steatosis (gray arrows). ABJ showed the best protective effects against AOM.

4. Discussion

The existing knowledge on the adverse side effects of drugs that have been proposed for the cancer treatments has stimulated extensive research aiming to search for natural choices that could reduce the amount of drug needed for cancer, not only as a chemoprotective event during the cancer process but also as chemopreventive products to avoid the cancer development (Cragg & Pezzuto, 2016). For this, natural food products such as berries could be a source of bioactive compounds with demonstrated anticancer effects due to synergistic effects between all of their components (May et al., 2020). As such, Andean berry (*Vaccinium meridionale* Swartz) offers the opportunity to include an underutilized fruit as a promising food matrix with the potential to alleviate chronic conditions (Quintero-Quiroz et al., 2019). Most studies involving Andean berry have focused on the use of the whole matrix, its juice, or derived food products for several applications such as hypolipidemic (Marín-Echeverri et al., 2018), hypoglycemic (Galvis-Pérez et al., 2020), antioxidant (Estupiñán-Amaya et al., 2020), and potentially chemopreventive *in vitro* (Agudelo et al., 2020; González et al., 2017). However, only a few studies have explored combined treatments with Aspirin, hypothesizing that Aspirin and ABJ combinations could reduce the Aspirin dosage to deliver even higher health benefits (Arango-Varela et al., 2020).

Several researchers have pointed out that ABJ benefits came from phenolic compounds, mainly phenolic acids and flavonoids (González et al., 2017; Shen et al., 2018). Some authors have highlighted that compounds such as delphinidin-3-hexoside, delphinidin-3-pentoside, cyanidin-3-galactoside, and cyanidin-3-arabinoside are the main anthocyanins from ABJ, while several caffeic acids, quercetin, and caffeoylquinic acid derivatives are the major non-anthocyanin phenolics found in Andean berry (Garzón et al., 2010). The amount of phenolic compounds identified in this study agrees with a previous polyphenolic characterization of ABJ for chlorogenic acid and its derivatives (Garzón et al., 2010), but 3,4-dihydroxybenzoic and 2-hydroxycinnamic have not been previously identified in ABJ nor *V. meridionale*-derived products. However, several hydroxycinnamic acids have been identified in berries, such as European cranberry (*Vaccinium oxycoccos*), representing the third most abundant group of phenolic compounds, after anthocyanins and flavonols (Jurikova et al., 2018).

Previously, the bioaccessibility of these compounds along the gastrointestinal tract was characterized, using a simulated gastrointestinal digestion procedure, where particularly ellagic, chlorogenic, gallic,

and caffeic acids were highly bioaccessible along with the digestion (>25 % bioaccessibility), suggesting that most of these compounds can reach metabolic targets to exert their health benefit (Agudelo et al., 2018). Moreover, in a recent study, Arango-Varela et al. (2020) found that gallic acid and cyanidin chloride were associated with the strongest health benefits in macrophages such as nitric oxide and intracellular reactive oxygen species (ROS) reductions and the decrease of pro-inflammatory cytokines such as IL-1 β and IL-1R, which agrees with the gallic acid activity over the nucleotide-binding oligomerization domain-like receptor 3 (NLRP3) inflammasome (Luzardo-Ocampo et al., 2020b). Moreover, as ABJ concentrations up to 50 % v/v showed no impact on the macrophages' cell viability (Arango-Varela et al., 2020), it is demonstrated that this treatment is not harmful to healthy cells, as macrophages have been used as a reference cell line to test materials' cytotoxicity (Park et al., 2015). Hence, 30 % v/v was selected as the maximum dose exhibiting antiproliferative effects without producing cytotoxic effects.

As shown by the cell viability tests, the longer the treatment was applied, the higher cytotoxic effect was shown, particularly for the ABJ and Aspirin combination. Similar to this study, Aspirin doses from 1.56 mM to 200 mM significantly ($p < 0.05$) decreased SW480 cell viability after 48 h treatment (Bagheri et al., 2020), whereas a previous study reported IC₅₀ values of 19, 8, and 3 % for 24, 48, and 72 h of treatment, respectively, for the same cell line (Agudelo et al., 2017). The cytotoxic effect of Aspirin has been attributed to its inhibitor activity on cyclooxygenase 2 (COX-2) and its incidence on the signal transducer and activator of transcription (STAT) signaling, and glycolysis and NF- κ B inhibition (Al-Nimer et al., 2015). There are no reports for the cloning efficiency for ABJ, but some reports have linked selected phenolic compounds with these properties. For instance, epigallocatechin gallate from green tea (0–25 μ M) decreased H1299 and H460 non-small cell lung cancer cells' ability to form colonies, compared to the untreated cells (Heyza et al., 2018). The authors explained the potential targeting of the proteasome, acting as chymotrypsin, trypsin, or peptidyl-glutamyl peptide hydrolyzing activities (Nabavi et al., 2018). Hydroxycinnamic acids have been targeted as strong antiproliferative compounds against colorectal cancer cells *in vitro*, a remarkable effect considering that these compounds are the main detectable colonic metabolites (Martini et al., 2019). Although the explored Aspirin doses in this research could be considered high, results are like other reports also using high Aspirin doses (5–20 mM) for several cancer cell lines (Dibra, Brown, Hooley, & Nicholl, 2010; Qin et al., 2013).

Cell cycle modulation is a target process from chemopreventive agents (Meeran, 2008). Results from this research suggest that Aspirin and ABJ treatments were cytostatic, in agreement with the induction of SW620 and SW480 cells transition to G0/G1 and G2/M phases after 48 and 72 h-treatments with Aspirin (1, 2.5, and 5 mM) (Gu et al., 2017). Regarding ABJ, reports have shown the impact of non-extractable polyphenols (16 μ g gallic acid equivalents/mL) from cranberries (*Vaccinium* subg. *Oxycoccus*) cv. Early Black such as procyanidin derivatives, quercetin, anthocyanins, *p*-coumaric acid, ferulic acid, chlorogenic acid, and caffeic acid, among other compounds, in cell cycle arrest (Han et al., 2019). Specifically, researchers observed an increase of HCT116 cell subpopulations in the G1 phase and decreased cells in the S phase compared to untreated cells. Similar effects were reported for chokeberry (*A. melanocarpa*) juice treatments (2 % v/v) of Caco-2 cells, showing a slow increase of cells at the G0/G1 phase and decrease of the S phase (Bermúdez-Soto et al., 2007).

Upon cell cycle arrest, caspase-3 mediates DNA damage and apoptosis induction under several mechanisms such as p21 cleavage or activation via extrinsic apoptosis (Mirzayans et al., 2016). On HCT116 human colorectal cancer cells, Aspirin (0.5 and 1 mM doses) has shown increased (1.65–1.90-fold, $p < 0.01$) caspase-3 activity compared to untreated cells, confirming the Aspirin-mediated pro-apoptotic induction involving a caspase-dependent pathway (Wang et al., 2015). Authors showed *in vivo* increase in cleaved-caspase-3 from whole cranberry

(*Vaccinium macrocarpon*) extract (WCE) administration to AOM/dextran sodium sulfate (DSS)-treated mice, in comparison to untreated mice, together with other pro-apoptotic markers such as p53 and cleaved poly (ADP-ribose) polymerase (PARP) expression (Wu et al., 2018). Moreover, WCE upregulated p21 and p27, while downregulated cyclin D1, CDK4, and the phosphorylation of retinoblastoma protein, essential proteins involved in cell cycle progression, leading to inhibition of cancer cell proliferation and growth. Although the authors did not inform about which components from WCE could be responsible for these effects, anthocyanin such as cyanidin-3-O-glucoside, cyanidin-3-O-galactoside, cyanidin-3-O-rutinoside, delphinidin-3-O-glucoside, among others, could impact the early caspase-3 activation in peripheral blood mononuclear cells (PBMCs) from patients with leukemia after a bilberry (*Vaccinium myrtillus*) administration (Alhosin et al., 2015).

A proteomic analysis was conducted to verify the expression of apoptosis-associated proteins due to Aspirin, ABJ, and their mixture. The obtained results from Aspirin confirmed its pro-apoptotic effect in SW480 cells due to the activation of pro-caspase-3, cleaved-caspase-3, and cytochrome C, favoring both extrinsic and intrinsic apoptotic pathways (M. Jiang et al., 2020). On the other hand, heat-shock proteins such as Hsp32 and Hsp70 block the apoptosome assembly, avoiding the development of the apoptotic process (Goloudina et al., 2012), suggesting a contradictory activity from Aspirin. However, Hsp70 has been found to present both pro- or anti-apoptotic mechanisms that should be evaluated independently on each living system since, for example, Hsp70 can over-activate certain immune receptors such as TLR4 and activate intracellular NF- κ B and STAT3 signaling in macrophages, extending a pro-inflammatory environment that could easily target cancer cells (Sharp et al., 2013). For the cells exposed to ABJ, its complex composition might activate several pro or anti-apoptotic mechanisms, where most pro-apoptotic signaling involving intrinsic and extrinsic pathways were activated (cytochrome C, SMAC, DIABLO, Bad; and apoptosis-related receptors: TNFRSF1A, TRAILR1, and TRAILR2). Few studies have evaluated the modulation of apoptosis-related proteins from *Vaccinium* fruits *in vitro* and *in vivo*. For example, an up-regulation of cleaved caspase-3, cleaved PARP, phospho-p53, and total Bad ($p < 0.05$) in SW480 cells treated with 8 % v/v ABJ was found, suggesting pro-apoptotic effects in this cell line (Agudelo et al., 2017). Commercial grape seed extracts (25–100 μ g/mL) containing procyanidins and monomeric flavonols found a significant increase of cytochrome C release, cleaved caspase-9, and cleaved caspase-3 on SW480, SW620, and HCT116 colorectal cancer cell lines, compared to the untreated cells (Derry et al., 2013). Activation of TRAIL pathways is notorious since CRC is particularly resistant to this activation (Deng & Shah, 2020). There are no reports of the joint effect of Aspirin and food matrices on the cancer treatment, but the mixture showed a profile where most proteins were decreased, indicating that a pro-apoptotic process does not mainly govern the antiproliferative and inhibitory effects of the mixture, but other mechanisms could be involved. For instance, catalase activation was observed to a minor extent, suggesting potential sensitization from cancer cells to oxidative stress, involving potential ROS generation that can lead to DNA-damage mechanisms (Glorieux et al., 2015). As observed by the bioinformatics analysis, p53 might be activated in the mixture and necroptosis, confirming this hypothesis. The ABJ chemical composition could be exerting this effect, as p53 is one of the main molecular targets of ellagic acid (González-Barrío et al., 2010). Downregulation of CDKN1A (p21 protein) indicates the ability of the mixture to inhibit apoptosis by impeding this protein to exert its reported inhibition of pro-caspase-3, caspase-8, caspase-10, the apoptosis signal-regulating kinase 1, and the stress-activated protein kinase (Kreis et al., 2019). The authors also reported the involvement of this protein in the cell cycle since its inhibition conducts to dysregulation of G2/M transition, resulting in mitotic defects and genomic instability of the cancer cell, agreeing with results from Fig. 3 where the mixture induced the lowest number of cells at this stage.

To potentially explain the involvement of Aspirin and ABJ in specific

apoptotic targets, *in silico* analyses were conducted, where the most promissory binding energies were selected. Aspirin showed the lowest binding energies among all the studied compounds. Nonetheless, the *in silico* analysis showed the highest affinity with p-RAD17, a fact that has been experimentally confirmed in HCT116 and HT-29, since Aspirin provokes phosphorylation of this protein at Ser465, inducing a p53-independent S-phase accumulation of these cells (Luciani et al., 2007). The ability of Aspirin to inhibit catalase has been reported as critical process to induce apoptosis in cancer cells since this process hinders reactive apoptosis-inducing intercellular ROS signaling of tumor (Scheit & Bauer, 2015). For all the other *in silico* analyses using ABJ components, catalase, Hsp70, and HIF-1 α were some of the shared targets of these compounds, complementing the proteomic analysis concerning alternative pro-apoptotic mechanisms. These interactions offer alternative research opportunities to detect molecular targets of ABJ compounds. Since proteins such as HIF-1 α are a high contributor to tumor aggressiveness and invasiveness and has been associated with basement membrane invasion and prolongation of tumorigenesis in HCT116 and SW480 colorectal cancer cells *in vitro* (Ioannou et al., 2015), future ABJ research in colorectal cancer could be benefited exploring these alternate mechanisms.

In vivo chemoprotective and chemopreventive assessment aims to consider both potential applications of phytochemicals could be more effective before the cancer progression or during the early stages of development (Koh et al., 2020). Based on the obtained results, early-stage carcinogenesis was obtained after the treatment with AOM since no significant differences were obtained in the bodyweight evolution between the groups, and slight reductions were observed from week 7.

Aberrant crypt foci have been recognized as neoplastic lesions, and therapeutic interventions aiming at its reduction are highly beneficial to avoid CRC progression (Wargovich et al., 2010). The significant ACF reduction by the Aspirin treatments agrees with 25 mg/kg Aspirin administration of AOM-treated FVB/N mice (Rohwer et al., 2020). For ABJ, ACF reduction could be associated with antioxidant mechanisms displayed by berries' phenolic compounds, involving the reduction of oxidative stress and DNA damage markers (Afrin et al., 2016). Mixtures of phenolic compounds such as gallic, ellagic, caffeic, and chlorogenic acids have shown synergistic antioxidant health benefits, contributing to protective mechanisms against AOM toxic effects. Other reports combining Aspirin with curcumin (0.01 % v/v + 1 % v/v) showed reductions in CRC tumor growth *in vivo* (C57BL/6 mice, 28-weeks treatment) in an AOM/DSS model due to beneficial effects of epigallocatechin gallate and Aspirin.

Due to the hepatotoxic effects of AOM, relative liver weight was evaluated. Although AOM-treated mice showed the lowest values, other researchers have found no impact of AOM on liver weight (Cuellar-Núñez et al., 2018), indicating that further histopathologic analysis is required. The H&E staining pictures showed early-stage carcinogenesis development in AOM-treated mice, mainly governed by increased cell infiltration and loss of colonic architecture, but the effects were similar in the chemoprotective and chemopreventive treatments. However, the treatments (Aspirin, ABJ, and their mixture) showed more beneficial effects in the chemopreventive evaluations. Decreased cell infiltration indirectly measured by colonic myeloperoxidase enzyme (MPO) has been observed after Açai (*Euterpe oleracea* Mart.) berry administration to AOM/DSS-treated ICR mice (Choi et al., 2017), in a process involving the reduction of pro-inflammatory cytokines (IL-1 β , TNF- α , and IL-6), pro-apoptotic mechanisms (cleaved-caspase-3 and Bad increase), and oxidative stress reductions (COX-2 decrease). The overall examination of the colon tissues indicated a higher impact of the chemopreventive approach in protecting the colon architecture from the AOM-induced damage. Phytochemicals from ABJ could act as chemopreventive agents, potentially inducing cell mechanisms that further avoid colon cancer development by decreasing the activation of related key pro-inflammatory mechanisms such as nuclear factor kappa B (NF- κ B) and PI3K-Akt pathways (Setia et al., 2014). This fact is supported by a recent

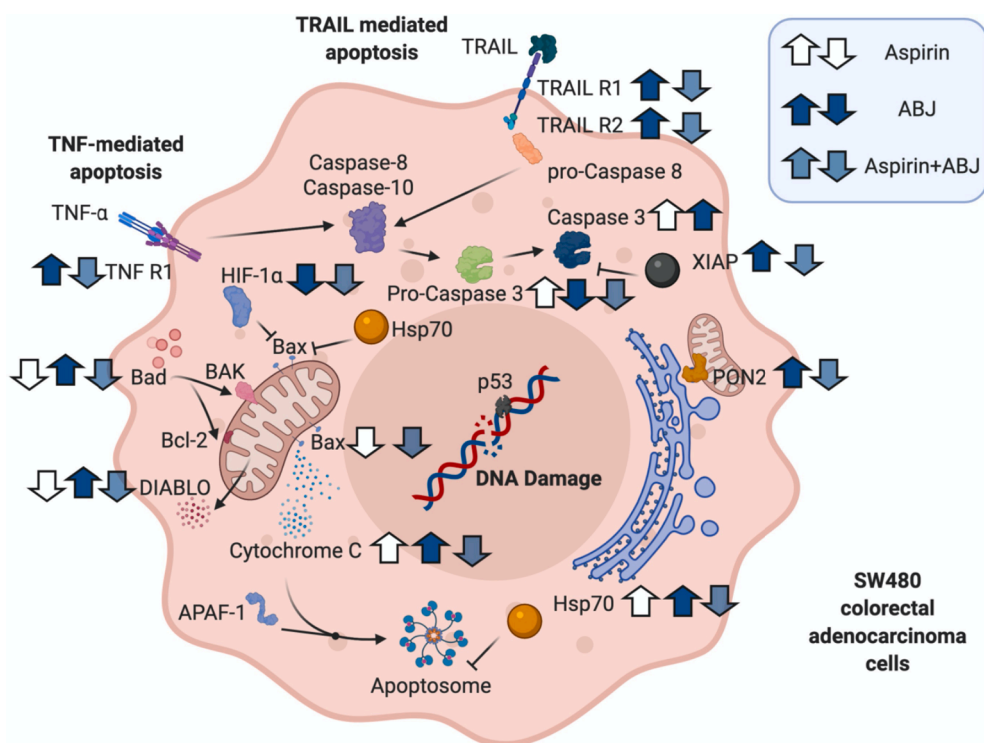


Fig. 9. Overall summary of the modulated pathways in SW480 cells by Aspirin, ABJ, and their mixture. The arrows indicate potential up-regulation or down-regulation of selected proteins. The graphic was done with [Biorender.com](https://www.biorender.com). ABJ: Andean berry juice.

article indicating the ability of ABJ to successfully reduce the production of pro-inflammatory cytokines such as TNF- α and IL-1 β in LPS-stimulated macrophages (Arango-Varela et al., 2020). In addition, the well-known inhibitory activity of Aspirin on COX-2 also regulates genes linked to cell growth, differentiation, and apoptosis, impeding further cancer development (Jalving et al., 2005).

An overall summary of the involved mechanisms is shown in Fig. 9. Aspirin treatment increased cytochrome C and pro-caspase-3 expressions and caspase-3 activity but inhibited Bad, DIABLO, and Bax, indicating the extrinsic pathway could mediate that. ABJ exhibited TRAIL-related apoptosis activation, whereas ABJ + Aspirin induced TNF-mediated apoptosis, potential cytochrome C release, and caspase-3 activity. Although these pathways were observed *in vitro*, results from the chemopreventive and chemoprotective approaches confirmed that ABJ components are exerting antiproliferative effects leading to the amelioration of colon cancer development.

5. Conclusion

In conclusion, this research suggested that ABJ and Aspirin mixture exhibited a higher antiproliferative effect on SW480 cells than the individual treatment of each. The mixture increased cell cycle arrest, modulated pro-apoptotic proteins, and suggested an alternative programmed cell death as suggested by the proteomic bioinformatics analyses. Results from the *in silico* analysis suggested a potential modulation of antioxidant, hypoxia, and receptor-mediated mechanisms by both ABJ and Aspirin, that could be used as future research targets assessing the impact of these treatments in colorectal cancer. These results were observed in an *in vivo* induction of early-stage carcinogenesis since the treatments preserved the colonic architecture. The combination of natural food products and commonly used drugs in cancer treatment, aiming to reduce drugs dosage and its side effects, could be an effective strategy to provide health benefits alleviating CRC risk. This study presents limitations as more human colorectal cancer cell lines should be assayed exhibited the different cycles of the cancer development.

Moreover, additional *in vivo* studies should be performed evaluating additional doses and potential extensive treatment times, together with transcriptomic analyses to fully understand the anti-proliferative and pro-apoptotic mechanisms derived from ABJ + Aspirin treatment.

Declaration of Competing Interest

The authors declare that they have no known competing financial interests or personal relationships that could have appeared to influence the work reported in this paper.

Acknowledgments

Author Sandra S. Arango appreciate the granted Ph.D. scholarship from Departamento Administrativo de Ciencia, Tecnología e Innovación – COLCIENCIAS (grant number: 7851) and Instituto Tecnológico Metropolitano (ITM), Medellín, Colombia. Author Ivan Luzardo-Ocampo acknowledges Programa de Becas Posdoctorales de la UNAM (DGAPA-CTIC) for his postdoctoral scholarship [grant number: 5267]. The support given by COLCIENCIAS through the Program Ecosistema Científico Cod. FP44842-211-2018 [project number: 58580] is well appreciated.

Appendix A. Supplementary material

Supplementary data to this article can be found online at <https://doi.org/10.1016/j.foodres.2022.111244>.

References

- Afrin, S., Giampieri, F., Gasparrini, M., Forbes-Hernandez, T., Varela-López, A., Quiles, J. L., Mezzetti, B., & Battino, M. (2016). Chemopreventive and therapeutic effects of edible berries: A focus on colon cancer prevention and treatment. *Molecules*, 21(2), 169. <https://doi.org/10.3390/molecules21020169>
- Agudelo, C. D., Arango, S., Cortés-mancera, F., Rojano, B., & Maldonado, M. E. (2017). Antiproliferative and pro-apoptotic effects of Andean berry juice (*Vaccinium meridionale* Swartz) on human colon adenocarcinoma SW480 cells. *Journal of*

- Medicinal Plants Research Full*, 11(24), 393–402. <https://doi.org/10.5897/JMPR2017.6401>
- Agudelo, C. D., Ceballos, N., Gómez-García, A., & Maldonado-Celis, M. E. (2018). Andean Berry (Vaccinium meridionale Swartz) juice improves plasma antioxidant capacity and IL-6 levels in healthy people with dietary risk factors for colorectal cancer. *Journal of Berry Research*, 8(4), 251–261. <https://doi.org/10.3233/JBR-180312>
- Agudelo, C. D., Luzardo-Ocampo, I., Campos-Vega, R., Loarca-Piña, G., & Maldonado-Celis, M. E. (2018). Bioaccessibility during in vitro digestion and antiproliferative effect of bioactive compounds from Andean berry (Vaccinium meridionale Swartz) juice. *Journal of Agricultural and Food Chemistry*, 66(28), 7358–7366. <https://doi.org/10.1021/acs.jafc.8b01604>
- Agudelo, C. D., Luzardo-Ocampo, I., Hernández-Arriaga, A. M., Rendón, J. C., Campos-Vega, R., & Maldonado-Celis, M. E. (2020). Fermented non-digestible fraction of andean berry (Vaccinium meridionale Swartz) juice induces apoptosis in colon adenocarcinoma cells. *Preventive Nutrition and Food Science*, 25(3), 272–279. <https://doi.org/10.3746/pnf.2020.25.3.272>
- Al-Nimer, M. S. M., Hameed, H. G., & Mahmood, M. M. (2015). Antiproliferative effects of aspirin and diclofenac against the growth of cancer and fibroblast cells: In vitro comparative study. *Saudi Pharmaceutical Journal*, 23(5), 483–486. <https://doi.org/10.1016/j.jsps.2015.01.002>
- Alhoshin, M., León-González, A. J., Dandache, I., Lelay, A., Rashid, S. K., Kevers, C., Pincemail, J., Fornecker, L.-M., Mauvieux, L., Herbrecht, R., & Schini-Kerth, V. B. (2015). Bilberry extract (Antho 50) selectively induces redox-sensitive caspase 3-related apoptosis in chronic lymphocytic leukemia cells by targeting the Bcl-2/Bad pathway. *Scientific Reports*, 5(1), 8996. <https://doi.org/10.1038/srep08996>
- Arango-Varela, S. S., Luzardo-Ocampo, I., Maldonado-Celis, M. E., & Campos-Vega, R. (2020). Andean berry (Vaccinium meridionale Swartz) juice in combination with Aspirin modulated anti-inflammatory markers on LPS-stimulated RAW 264.7 macrophages. *Food Research International*, 137, Article 109541. <https://doi.org/10.1016/j.foodres.2020.109541>
- Baby, B., Antony, P., & Vijayan, R. (2018). Antioxidant and anticancer properties of berries. *Critical Reviews in Food Science and Nutrition*, 58(15), 2491–2507. <https://doi.org/10.1080/10408398.2017.1329198>
- Bagheri, M., Tabatabaei Far, M. A., Mirzaei, H., & Ghasemi, F. (2020). Evaluation of antitumor effects of aspirin and LGK974 drugs on cellular signaling pathways, cell cycle and apoptosis in colorectal cancer cell lines compared to oxaliplatin drug. *Fundamental & Clinical Pharmacology*, 34(1), 51–64. <https://doi.org/10.1111/fcp.12492>
- Bermúdez-Soto, M., Larrosa, M., García-Cantalejo, J. M., Espín, J. C., Tomás-Barberán, F. A., & García-Conesa, M. T. (2007). Up-regulation of tumor suppressor carcinoembryonic antigen-related cell adhesion molecule 1 in human colon cancer Caco-2 cells following repetitive exposure to dietary levels of a polyphenol-rich chokeberry juice. *The Journal of Nutritional Biochemistry*, 18(4), 259–271. <https://doi.org/10.1016/j.jnutbio.2006.05.003>
- Biasini, M., Bienert, S., Waterhouse, A., Arnold, K., Studer, G., Schmidt, T., Kiefer, F., Cassarino, T. G., Bertoni, M., Bordoli, L., & Schwede, T. (2014). SWISS-MODEL: Modelling protein tertiary and quaternary structure using evolutionary information. *Nucleic Acids Research*, 42(W1), W252–W258. <https://doi.org/10.1093/nar/gku340>
- Choi, Y. J., Choi, Y. J., Kim, N., Nam, R. H., Lee, S., Lee, H. S., Lee, H.-N., Surh, Y.-J., & Lee, D. H. (2017). Açaí berries inhibit colon tumorigenesis in azoxymethane/dextran sulfate sodium-treated mice. *Gut and Liver*, 11(2), 243–252. <https://doi.org/10.5009/gnl16068>
- Cragg, G. M., & Pezzuto, J. M. (2016). Natural products as a vital source for the discovery of cancer chemotherapeutic and chemopreventive agents. *Medical Principles and Practice*, 25(2), 41–59. <https://doi.org/10.1159/000443404>
- Cuellar-Núñez, M. L., Luzardo-Ocampo, I., Campos-Vega, R., Gallegos-Corona, M. A., González de Mejía, E., & Loarca-Piña, G. (2018). Physicochemical and nutraceutical properties of moringa (Moringa oleifera) leaves and their effects in an in vivo AOM/DSS-induced colorectal carcinogenesis model. *Food Research International*, 105(C), 159–168. <https://doi.org/10.1016/j.foodres.2017.11.004>
- D'Archivio, M., Santangelo, C., Scaccocchio, B., Vari, R., Filesi, C., Masella, R., & Giovannini, C. (2008). Modulatory effects of polyphenols on apoptosis induction: Relevance for cancer prevention. *International Journal of Molecular Sciences*, 9(3), 213–228. <https://doi.org/10.3390/ijms9030213>
- Deng, D., & Shah, K. (2020). TRAIL of hope meeting resistance in cancer. *Trends in Cancer*, 6(12), 989–1001. <https://doi.org/10.1016/j.trecan.2020.06.006>
- Derry, M., Raina, K., Agarwal, R., & Agarwal, C. (2013). Differential effects of grape seed extract against human colorectal cancer cell lines: The intricate role of death receptors and mitochondria. *Cancer Letters*, 334(1), 69–78. <https://doi.org/10.1016/j.canlet.2012.12.015>
- Dibra, H., Brown, J. E., Hooley, P., & Nicholl, I. D. (2010). Aspirin and alterations in DNA repair proteins in the SW480 colorectal cancer cell line. *Oncology Reports*, 24(1), 37–46. <https://doi.org/10.3892/or.00000826>
- Drew, D. A., Cao, Y., & Chan, A. T. (2016). Aspirin and colorectal cancer: The promise of precision chemoprevention. *Nature Reviews Cancer*, 16(3), 173–186. <https://doi.org/10.1038/nrc.2016.4>
- Estupiñán-Amaya, M., Fuenmayor, C. A., & López-Córdoba, A. (2020). New freeze-dried andean blueberry juice powders for potential application as functional food ingredients: Effect of maltodextrin on bioactive and morphological features. *Molecules*, 25(23), 5635. <https://doi.org/10.3390/molecules25235635>
- Franco-Tobón, Y. N., Rojano, B. A., Alzate Arbeláez, A. F., Morales Saavedra, D. M., Maldonado-Celis, M. E., Franco, Y., Rojano, B. A., Alzate, A., Restrepo, C., Rivero, D., & Maldonado, M. (2016). Efecto del tiempo de almacenamiento sobre propiedades fisicoquímicas y antioxidantes de productos derivados del fruto agraz (Vaccinium meridionale swartz). *Archivos Latinoamericanos de Nutrición*, 23(4), 261–271. <http://www.alanrevista.org/ediciones/2016/4/art-1/>
- Franken, N. A. P., Rodermond, H. M., Stap, J., Haveman, J., & van Bree, C. (2006). Clonogenic assay of cells in vitro. *Nature Protocols*, 1(5), 2315–2319. <https://doi.org/10.1038/nprot.2006.339>
- Galvis-Pérez, Y., Marín-Echeverri, C., Franco Escobar, C. P., Aristizábal, J. C., Fernández, M.-L., & Barona-Acevedo, J. (2020). Comparative evaluation of the effects of consumption of colombian Agraz (Vaccinium meridionale Swartz) on insulin resistance, antioxidant capacity, and markers of oxidation and inflammation, between men and women with metabolic syndrome. *BioResearch Open Access*, 9(1), 247–254. <https://doi.org/10.1089/biores.2020.0053>
- Garzón, G. A. (2012). Colombian bilberry (Vaccinium meridionale Swartz): Chemical composition, antioxidant activity, anthocyanin and non-anthocyanin phenolic composition as compared to other Vaccinium species. In C. Tuberoso (Ed.), *Berries: Properties, Consumption and Nutrition* (Issue November, pp. 157–167). Nova Science Publishers, Inc. <https://doi.org/10.13140/2.1.3987.1685>
- Garzón, G. A., Narváez, C. E., Riedl, K. M., & Schwartz, S. J. (2010). Chemical composition, anthocyanins, non-anthocyanin phenolics and antioxidant activity of wild bilberry (Vaccinium meridionale Swartz) from Colombia. *Food Chemistry*, 122(4), 980–986. <https://doi.org/10.1016/j.foodchem.2010.03.017>
- Glorieux, C., Zamocky, M., Sandoval, J. M., Verrax, J., & Calderon, P. B. (2015). Regulation of catalase expression in healthy and cancerous cells. *Free Radical Biology and Medicine*, 87, 84–97. <https://doi.org/10.1016/j.freeradbiomed.2015.06.017>
- Goldar, S., Khaniani, M. S., Derakhshan, S. M., & Baradaran, B. (2015). Molecular mechanisms of apoptosis and roles in cancer development and treatment. *Asian Pacific Journal of Cancer Prevention*, 16(6), 2129–2144. <https://doi.org/10.7314/APJCP.2015.16.6.2129>
- Goloudina, A. R., Demidov, O. N., & Garrido, C. (2012). Inhibition of HSP70: A challenging anti-cancer strategy. *Cancer Letters*, 325(2), 117–124. <https://doi.org/10.1016/j.canlet.2012.06.003>
- González-Barrio, R., Borges, G., Mullen, W., & Crozier, A. (2010). Bioavailability of anthocyanins and ellagitannins following consumption of raspberries by healthy humans and subjects with an ileostomy. *Journal of Agricultural and Food Chemistry*, 58(7), 3933–3939. <https://doi.org/10.1021/jf1000315d>
- González, M., Samudio, I., Sequeda-Castañeda, L. G., Celis, C., Iglesias, J., & Morales, L. (2017). Cytotoxic and antioxidant capacity of extracts from Vaccinium meridionale Swartz (Ericaceae) in transformed leukemic cell lines. *Journal of Applied Pharmaceutical Science*, 7(3), 24–30. <https://doi.org/10.7324/JAPS.2017.70305>
- Gu, M., Nishihara, R., Chen, Y., Li, W., Shi, Y., Masugi, Y., Hamada, T., Kosumi, K., Liu, L., Silva, A., Nowak, J. A., Twombly, T., Du, C., Koh, H., Li, W., Meyerhardt, J. A., Wolpin, B. M., Giannakis, M., & Aguirre, A. J. (2017). Aspirin exerts high anti-cancer activity in PIK3CA-mutant colon cancer cells. 8(50), 87379–87389.
- Han, Y., Huang, M., Li, L., Cai, X., Gao, Z., Li, F., Rakariyatham, K., Song, M., Fernández Tomé, S., & Xiao, H. (2019). Non-extractable polyphenols from cranberries: Potential anti-inflammation and anti-colon-cancer agents. *Food & Function*, 10(12), 7714–7723. <https://doi.org/10.1039/C9FO01536A>
- Heyza, J., Arora, S., Zhang, H., Conner, K., Lei, W., Floyd, A., Deshmukh, R., Sarver, J., Trabbic, C., Erhardt, P., Chan, T.-H., Dou, Q., & Patrick, S. (2018). Targeting the DNA repair endonuclease ERCC1-XPF with green tea polyphenol epigallocatechin-3-gallate (EGCG) and its prodrug to enhance cisplatin efficacy in human cancer cells. *Nutrients*, 10(11), 1644. <https://doi.org/10.3390/nu10111644>
- Ioannou, M., Paraskeva, E., Baxevedinou, K., Simos, G., Papamichali, R., Papacharalambous, C., Samara, M., & Koukolis, G. (2015). HIF-1α in colorectal carcinoma: Review of literature. *Journal of the Balkan Union of Oncology*, 20(3), 680–689.
- Jalving, M., Koomstra, J. J., Jong, S., Vries, E. G. E., & Kleibeuker, J. H. (2005). Review article: The potential of combinational regimen with non-steroidal anti-inflammatory drugs in the chemoprevention of colorectal cancer. *Alimentary Pharmacology and Therapeutics*, 21(4), 321–339. <https://doi.org/10.1111/j.1365-2036.2005.02335.x>
- Jiang, M., Qi, L., Li, L., & Li, Y. (2020). The caspase-3/GSDME signal pathway as a switch between apoptosis and pyroptosis in cancer. *Cell Death Discovery*, 6(1). <https://doi.org/10.1038/s41420-020-00349-0>
- Jiang, W., Yan, Y., Chen, M., Luo, G., Hao, J., Pan, J., Hu, S., Guo, P., Li, W., Wang, R., Zuo, Y., Sun, Y., Sui, S., Yu, W., Pan, Z., Zou, K., Zheng, Z., Deng, W., Wu, X., & Guo, W. (2020). Aspirin enhances the sensitivity of colon cancer cells to cisplatin by abrogating the binding of NF-κB to the COX-2 promoter. *Aging*, 12(1), 611–627. <https://doi.org/10.18632/aging.102644>
- Jingwen, B., Yaochen, L., & Guojun, Z. (2017). Cell cycle regulation and anticancer drug discovery. *Cancer Biology & Medicine*, 14(4), 348. <https://doi.org/10.20892/j.issn.2095-3941.2017.0033>
- Jurikova, T., Skrovankova, S., Mlcek, J., Balla, S., & Snopek, L. (2018). Bioactive compounds, antioxidant activity, and biological effects of European cranberry (Vaccinium oxycoccos). *Molecules*, 24(1), 24. <https://doi.org/10.3390/molecules24010024>
- Koh, Y.-C., Ho, C.-T., & Pan, M.-H. (2020). Recent advances in cancer chemoprevention with phytochemicals. *Journal of Food and Drug Analysis*, 28(1), 14–37. <https://doi.org/10.1016/j.jfda.2019.11.001>
- Kreis, Louwen, & Yuan. (2019). The Multifaceted p21 (Cip1/Waf1/CDKN1A) in cell differentiation, migration and cancer therapy. *Cancers*, 11(9), 1220. <https://doi.org/10.3390/cancers11091220>
- Landis-piwowar, K. R., & Iyer, N. R. (2014). Cancer chemoprevention: Current state of the art. *Cancer Growth and Metastasis*, 7, 19–25. <https://doi.org/10.4137/CGM.S11288.RECEIVED>
- Ligarreto, G. A., del Patiño, M., & Magnitskiy, S. V. (2011). Phenotypic plasticity of Vaccinium meridionale (Ericaceae) in wild populations of mountain forests in Colombia. *Revista de Biología Tropical*, 59(2), 569–583.

- López, P. J. T., Alberó, J. S., & Rodríguez-Montes, J. A. (2014). Primary and secondary prevention of colorectal cancer. *Clinical Medicine Insights: Gastroenterology*, 7. <https://doi.org/10.4137/CGast.S14039>. CGast.S14039.
- Luciani, M. G., Campregheer, C., Fortune, J. M., Kunkel, T. A., & Gasche, C. (2007). 5-ASA affects cell cycle progression in colorectal cells by reversibly activating a replication checkpoint. *Gastroenterology*, 132(1), 221–235. <https://doi.org/10.1053/j.gastro.2006.10.016>
- Luna-Vital, D., Weiss, M., & Gonzalez de Mejia, E. (2017). Anthocyanins from purple corn ameliorated Tumor Necrosis Factor- α -induced inflammation and insulin resistance in 3T3-L1 adipocytes via activation of insulin signaling and enhanced GLUT4 translocation. *Molecular Nutrition and Food Research*, 61(12), 1–13. <https://doi.org/10.1002/mnfr.201700362>
- Luzardo-Ocampo, I., Campos-Vega, R., Cuellar-Núñez, M. L. L., Vázquez-Landaverde, P. A. A., Mojica, L., Acosta-Gallegos, J. A. A., & Loarca-Piña, G. (2018). Fermented non-digestible fraction from combined nixtamalized corn (*Zea mays* L.) / cooked common bean (*Phaseolus vulgaris* L.) chips modulate anti-inflammatory markers on RAW 264.7 macrophages. *Food Chemistry*, 259(C), 7–17. <https://doi.org/10.1016/j.foodchem.2018.03.096>
- Luzardo-Ocampo, I., Campos-Vega, R., Gonzalez de Mejia, E., & Loarca-Piña, G. (2020a). Consumption of a baked corn and bean snack reduced chronic colitis inflammation in CD-1 mice via downregulation of IL-1 receptor, TLR, and TNF- α associated pathways. *Food Research International*, 132(C), Article 109097. <https://doi.org/10.1016/j.foodres.2020.109097>
- Luzardo-Ocampo, I., Loarca-Piña, G., & Gonzalez de Mejia, E. (2020b). Gallic and butyric acids modulated NLRP3 inflammasome markers in a co-culture model of intestinal inflammation. *Food and Chemical Toxicology*, 146, Article 111835. <https://doi.org/10.1016/j.fct.2020.111835>
- Maldonado-Celis, M. E., Franco-Tobón, Y. N., Agudelo, C., Arango, S. S., & Rojano, B. (2017). Andean Berry (*Vaccinium meridionale Swartz*). In E. M. Yahia (Ed.), *Fruit and Vegetable Phytochemicals* (First, pp. 869–882). John Wiley & Sons, Ltd. <https://doi.org/10.1002/9781119158042.ch40>
- Marín-Echeverri, C., Blesso, C., Fernández, M., Galvis-Pérez, Y., Ciro-Gómez, G., Núñez-Rangel, V., Aristizábal, J., & Barona-Acevedo, J. (2018). Effect of agraz (*Vaccinium meridionale Swartz*) on high-density lipoprotein function and inflammation in women with metabolic syndrome. *Antioxidants*, 7(12), 185. <https://doi.org/10.3390/antiox7120185>
- Martini, S., Conte, A., & Tagliazucchi, D. (2019). Antiproliferative Activity and Cell Metabolism of Hydroxycinnamic Acids in Human Colon Adenocarcinoma Cell Lines. *Journal of Agricultural and Food Chemistry*, 67(14), 3919–3931. <https://doi.org/10.1021/acs.jafc.9b00522>
- Mattiuzzi, C., Sanchis-Gomar, F., & Lippi, G. (2019). Concise update on colorectal cancer epidemiology. *Annals of Translational Medicine*, 7(21). <https://doi.org/10.21037/atm.2019.07.91>
- May, S., Parry, C., & Parry, L. (2020). Berry chemoprevention: Do berries decrease the window of opportunity for tumorigenesis. *Food Frontiers*, 1(3), 260–275. <https://doi.org/10.1002/fft2.32>
- Meeran, S. M. (2008). Cell cycle control as a basis for cancer chemoprevention through dietary agents. *Frontiers in Bioscience*, 13(13), 2191. <https://doi.org/10.2741/2834>
- Mirzayans, R., Andrais, B., Kumar, P., & Murray, D. (2016). The Growing complexity of cancer cell response to DNA-damaging agents: Caspase 3 mediates cell death or survival? *International Journal of Molecular Sciences*, 17(5), 708. <https://doi.org/10.3390/ijms17050708>
- Nabavi, S. F., Atanasov, A. G., Khan, H., Barreca, D., Trombetta, D., Testai, L., Sureda, A., Tejada, S., Vacca, R. A., Pittalà, V., Gulei, D., Berindan-Neagoe, I., Shirooie, S., & Nabavi, S. M. (2018). Targeting ubiquitin-proteasome pathway by natural, in particular polyphenols, anticancer agents: Lessons learned from clinical trials. *Cancer Letters*, 434, 101–113. <https://doi.org/10.1016/j.canlet.2018.07.018>
- Orlando, F. A., Tan, D., Baltodano, J. D., Khoury, T., Gibbs, J. F., Hassid, V. J., Ahmed, B. H., & Alrawi, S. J. (2008). Aberrant crypt foci as precursors in colorectal cancer progression. *Journal of Surgical Oncology*, 98(3), 207–213. <https://doi.org/10.1002/jso.21106>
- Park, C. S., Choi, K. S., Park, I. W., Jung, J. W., Choi, J. C., Kim, J. Y., Choi, B. W., Kim, Y. G., Shin, J. W., & Kim, S. Y. (2015). Autophagy in RAW264.7 cells treated with surface-functionalized graphene oxides. *Journal of Nanomaterials*, 2015, 1–8. <https://doi.org/10.1155/2015/704789>
- Patra, S., Pradhan, B., Nayak, R., Behera, C., Rout, L., Jena, M., Efferth, T., & Bhutia, S. K. (2021). Chemotherapeutic efficacy of curcumin and resveratrol against cancer: Chemoprevention, chemoprotection, drug synergism and clinical pharmacokinetics. *Seminars in Cancer Biology*, 73, 310–320. <https://doi.org/10.1016/j.semcancer.2020.10.010>
- Quintero-Quiroz, J., Galvis-pérez, Y., Galeano-Vázquez, S., Marín-Echeverry, C., Franco-Escobar, C., Ciro-gómez, G., ... Ciro-Yong, G. (2019). Physico-chemical characterization and antioxidant capacity of the colombian berry (*Vaccinium meridionale Swartz*) with a high-polyphenol content: Potential effects in people with metabolic syndrome. *Food Science and Technology*, 39(3), 573–582. <https://doi.org/10.1590/fst.32817>
- Raju, J. (2008). Azoxy methane-induced rat aberrant crypt foci: Relevance in studying chemoprevention of colon cancer. *World Journal of Gastroenterology*, 14(43), 6632–6635. <https://doi.org/10.3748/wjg.14.6632>
- Ramírez-Jiménez, A. K., Reynoso-Camacho, R., Mendoza-Díaz, S., & Loarca-Piña, G. (2014). Functional and technological potential of dehydrated *Phaseolus vulgaris* L. flours. *Food Chemistry*, 161, 254–260. <https://doi.org/10.1016/j.foodchem.2014.04.008>
- Ramirez, V., Arango, S. S., Maldonado, M. E., Uribe, D., Aguillon, J., & Quintero, J. P. (2019). Biological activity of *Passiflora edulis* f. *Flavicarpa* ethanolic leaves extract on human colonic adenocarcinoma cells. *Journal of Applied Pharmaceutical Science*, 9(2), 64–71. <https://doi.org/10.7324/JAPS.2019.90209>
- Rohwer, N., Kühl, A. A., Ostermann, A. I., Hartung, N. M., Schebb, N. H., Zopf, D., McDonald, F. M., & Weylandt, K. H. (2020). Effects of chronic low-dose aspirin treatment on tumor prevention in three mouse models of intestinal tumorigenesis. *Cancer Medicine*, 9(7), 2535–2550. <https://doi.org/10.1002/cam4.2881>
- Scheit, K., & Bauer, G. (2015). Direct and indirect inactivation of tumor cell protective catalase by salicylic acid and anthocyanidins reactivates intercellular ROS signaling and allows for synergistic effects. *Carcinogenesis*, 36(3), 400–411. <https://doi.org/10.1093/carcin/bgv010>
- Setia, S., Nehru, B., & Sanyal, S. N. (2014). The PI3K/Akt pathway in colitis associated colon cancer and its chemoprevention with celecoxib, a Cox-2 selective inhibitor. *Biomedicine & Pharmacotherapy*, 68(6), 721–727. <https://doi.org/10.1016/j.biopha.2014.07.006>
- Sharma, V. K., Mamontov, E., & Tyagi, M. (2020). Effects of NSAIDs on the nanoscopic dynamics of lipid membrane. *Biochimica et Biophysica Acta (BBA) - Biomembranes*, 1862(2), Article 183100. <https://doi.org/10.1016/j.bbame.2019.183100>
- Sharp, F. R., Zhan, X., & Liu, D.-Z. (2013). Heat shock proteins in the brain: Role of Hsp70, Hsp27, and HO-1 (Hsp32) and their therapeutic potential. *Translational Stroke Research*, 4(6), 685–692. <https://doi.org/10.1007/s12975-013-0271-4>
- Shen, M., Li, K., Jing, H., & Zheng, L. (2018). In vivo therapeutic effect of *Vaccinium meridionale Swartz* in ischemia-reperfusion induced male albino rats. *Journal of Food Science*, 83(1), 221–228. <https://doi.org/10.1111/1750-3841.13986>
- Suzuki, R., Kohno, H., Sugie, S., Nakagama, H., & Tanaka, T. (2006). Strain differences in the susceptibility to azoxymethane and dextran sodium sulfate-induced colon carcinogenesis in mice. *Carcinogenesis*, 27(1), 162–169. <https://doi.org/10.1093/carcin/bgi205>
- Szliszka, E., & Krol, W. (2011). The role of dietary polyphenols in tumor necrosis factor-related apoptosis inducing ligand (TRAIL)-induced apoptosis for cancer chemoprevention. *European Journal of Cancer Prevention*, 20(1), 63–69. <https://doi.org/10.1097/CEJ.0b013e32833ecc48>
- Trott, O., & Olson, A. J. (2010). AutoDock Vina: Improving the speed and accuracy of docking with a new scoring function, efficient optimization, and multithreading. *Journal of Computational Chemistry*, 31(2), 455–461. <https://doi.org/10.1002/jcc.21334>
- Vichai, V., & Kirtikara, K. (2006). Sulforhodamine B colorimetric assay for cytotoxicity screening. *Nature Protocols*, 1(3), 1112–1116. <https://doi.org/10.1038/nprot.2006.179>
- von Mering, C., Jensen, L. J., Kuhn, M., Chaffron, S., Doerks, T., Kruger, B., Snel, B., Bork, P., Krüger, B., Snel, B., & Bork, P. (2007). STRING 7 - Recent developments in the integration and prediction of protein interactions. *Nucleic Acids Research*, 35(1), 358–362. <https://doi.org/10.1093/nar/gkl825>
- Wang, X., Diaoy, Y., Liu, Y., Gao, N., Gao, D., Wan, Y., Zhong, J., & Jin, G. (2015). Synergistic apoptosis-inducing effect of aspirin and isosorbide mononitrate on human colon cancer cells. *Molecular Medicine Reports*, 12(3), 4750–4758. <https://doi.org/10.3892/mmr.2015.3963>
- Wargovich, M. J., Brown, V. R., & Morris, J. (2010). Aberrant crypt foci: The case for inclusion as a biomarker for colon cancer. *Cancers*, 2(3), 1705–1716. <https://doi.org/10.3390/cancers2031705>
- Wong, M. C. S., Huang, J., Lok, V., Wang, J., Fung, F., Ding, H., & Zheng, Z.-J. (2021). Differences in incidence and mortality trends of colorectal cancer worldwide based on sex, age, and anatomic location. *Clinical Gastroenterology and Hepatology*, 19(5), 955–966.e61. <https://doi.org/10.1016/j.cgh.2020.02.026>
- Wu, X., Song, M., Cai, X., Neto, C., Tata, A., Han, Y., Wang, Q., Tang, Z., & Xiao, H. (2018). Chemopreventive effects of whole cranberry (*Vaccinium macrocarpon*) on colitis-associated colon tumorigenesis. *Molecular Nutrition & Food Research*, 62(24), 1800942. <https://doi.org/10.1002/mnfr.201800942>
- Ying, J., Zhou, H., Liu, P., You, Q., Kuang, F., Shen, Y., & Hu, Z. (2018). Aspirin inhibited the metastasis of colon cancer cells by inhibiting the expression of toll-like receptor 4. *Cell & Bioscience*, 8(1), 1. <https://doi.org/10.1186/s13578-017-0198-7>
- Zapata, I. C., Ochoa, S., Alzate, A. F., Zapata, A. D., & Rojano, B. A. (2020). Vinegar of Andean berries (*Vaccinium Meridionale SW*): Antioxidant and antiproliferative activity in colon cancer cells SW480. *Vitae*, 26(3), 135–147. <https://doi.org/10.17533/udea.vitae.v26n3a02>